HOMOGENIZATION OF QUASI-STATIC MAXWELL'S EQUATIONS

XUE JIANG* AND WEIYING ZHENG†

Abstract. This paper studies the homogenization of quasi-static and nonlinear Maxwell's equations in grain-oriented (GO) silicon steel laminations. GO silicon steel laminations have multiple scales and the ratio of the largest scale to the smallest scale can be up to 10^6. Direct solution of three-dimensional nonlinear Maxwell's equations is very challenging and unrealistic for large electromagnetic devices. Based on the magnetic vector potential and the magnetic field respectively, we propose two macro-scale models for the quasi-static Maxwell's equations. We prove that the micro-scale solutions converge to the solutions of the macro-scale models weakly in $\boldsymbol{H}(\mathbf{curl}, \Omega)$ and strongly in $\boldsymbol{L}^2(\Omega)$ as the thickness of lamination tends to zero. The wellposedness of the homogenized model is established by using weighted norms. Numerical experiments are carried out for a benchmark problem from the International Compumag Society, TEAM Workshop Problem 21^c–M1. The numerical results show good agreements with the experimental data and validate the homogenized model.

Key words. Homogenization, Maxwell's equations, eddy current, finite element method, grain-oriented silicon steel lamination

AMS subject classifications. 35K55, 65N30, 78A25

1. Introduction.

Quasi-static Maxwell's equations are widely used in electric engineering, such as large power transformers and electric generators, etc. The model neglects the displacement current density in Ampere's law and approximates the Maxwell's equations at very low frequency [1]:

$$\frac{\partial \boldsymbol{B}}{\partial t} + \mathbf{curl}\, \boldsymbol{E} = 0 \quad \text{in } \mathbb{R}^3, \qquad \text{(Farady's law)} \tag{1.1a}$$

$$\mathbf{curl}\, \boldsymbol{H} = \boldsymbol{J} \quad \text{in } \mathbb{R}^3, \qquad \text{(Ampere's law)} \tag{1.1b}$$

where $\boldsymbol{E}$ is the electric field, $\boldsymbol{B}$ is the magnetic flux density and $\boldsymbol{H}$ is the magnetic field. For simplicity, we neglect conduction current and only consider source current in coils. Let $\Omega_c = \text{supp}(\sigma)$ be the combination of conductors. Then the current density $\boldsymbol{J}$ is defined by:

$$\boldsymbol{J} = \begin{cases} \sigma \boldsymbol{E} & \text{in } \Omega_c, \\ \boldsymbol{J}_s & \text{in } \mathbb{R}^3 \backslash \bar{\Omega}_c, \end{cases} \tag{1.2}$$

where $\sigma \geq 0$ is the electric conductivity and $\boldsymbol{J}_s$ denotes the source current density carried by coils. Clearly we have

$$\text{supp}(\boldsymbol{J}_s) \cap \bar{\Omega}_c = \emptyset. \tag{1.3}$$

We are interested in grain-oriented (GO) silicon steel laminations where $\boldsymbol{B}$ is a nonlinear vector function of $\boldsymbol{H}$ and will be specified in more detail in the next section. In fact, (1.1) is also called electromagnetic eddy current problem in the engineering community.

*Academy of Mathematics and System Sciences, Super-computing Center, Computer Network Information Center, Chinese Academy of Sciences, Beijing, 100190, China. (jxue@lsec.cc.ac.cn)

†NCMIS, LSEC, Academy of Mathematics and System Sciences, Chinese Academy of Sciences, Beijing, 100190, China. The second author was supported in part by China NSF grants 11031006 and 11171334, by the Funds for Creative Research Groups of China 11021101, by National 863 Project of China under the grant 2012AA01A309, and by the National Magnetic Confinement Fusion Science Program 2011GB105003. (zwy@lsec.cc.ac.cn)

In this paper, we shall study the homogenization of (1.1) for GO silicon steel laminations which are widely used in iron cores and magnetic shields of large power transformers (see Fig. 1.1 for a laboratory model). The lamination stack consists of many steel sheets and has multiple scales. The ratio of the largest scale to the smallest scale can be up to 10^6. The length and width of each lamination are usually several meters and the thickness ϵ is about 0.18-0.35mm. Moreover, each steel sheet is coated with a thin layer of insulating film whose thickness is only 2-5μm. The coating films prevent electric currents from flowing into neighboring sheets, as seen in Figure 1.2. Full three-dimensional (3D) finite element simulation is extremely difficult due to extensive unknowns from meshing both laminations and coating films. Recently, Zheng et al proposed to compute 3D eddy currents in steel laminations by omitting coating films [19, 22, 29]. The scale ratio of the system is reduced from 10^6 to 10^4. They proved that the approximate solutions converge to the solution of (1.1) strongly in $\boldsymbol{L}^2(0,T;\boldsymbol{L}^2(\Omega))$. But the small parameter ϵ still remains and makes the simulation of large electromagnetic devices very difficult.

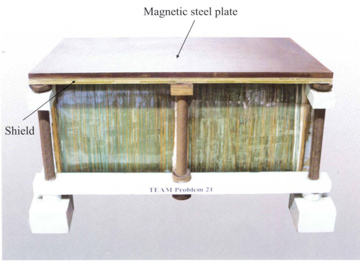

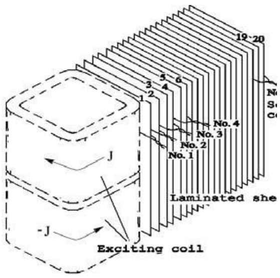

Fig. 1.1. *GO silicon steel laminations. (Left) the magnetic shield for protecting the magnetic plate; (Right) the magnetic shield made of laminated steel sheets.*

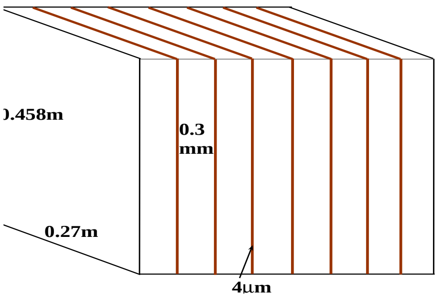

Fig. 1.2. *Geometric sizes of the silicon steel laminations.*

There are many works in the literature studying efficient numerical methods for linear eddy current problems. In 2000, Beck et al proposed a residual-based a posteriori error estimate for edge element approximation of eddy current problems [4]. They proved the reliability and efficiency of the a posteriori error estimate with respect to the approximation error in the energy norm. In 2006, Zheng et al proposed an adaptive finite element method for the $\boldsymbol{H}$-ψ formulation of time-dependent eddy current problems with multiply-connected conductors. Both the temporal and spatial meshes are refined or coarsened under reliable and efficient a posteriori error estimates [28]. In 2010, Chen et al studied the adaptive finite element method for eddy current model with circuit/field couplings [12]. In 2002, Hiptmair studied multigrid method for edge element discretization of eddy current problems [18]. In 2010, Ledger and Zaglmayr computed eddy current problems on multiply-connected domains by hp-finite element method and proposed an efficient solver for the discrete problem [21]. In 2003, Costabel et al studied the regularity of the solution of eddy current problems [13]. However, mathematical and numerical theories for nonlinear eddy current problems are rather rare in the literature. Here we refer to Bachinger et al [3] for the numerical analysis of nonlinear multi-harmonic eddy current problems in isotropic materials.

However, in the engineering community, there are considerable efforts in developing efficient numerical methods for nonlinear eddy current problems for sillicon steel laminations [11]. Most of them resort to replace physical parameters with effective parameters in Maxwell's equations, such as permeability and electric conductivity [5, 6, 20, 25]. In [7, 8], Bottauscio et al proposed a mathematical homogenization technique based on multi-scale expansion theory to derive equivalent electric parameters and effective magnetization properties. In [14, 15], Gyselinck et al deduced effective material parameters by an orthogonal decomposition of the magnetic flux density in the perpendicular and parallel directions to the lamination plane. In [17], Napieralska-Juszczak et al established equivalent characteristics of magnetic joints of transformer cores by minimizing the magnetic energy of the system. Numerical methods based on the homogenization of material parameters provide an efficient way to simulate electromagnetic fields in steel laminations. In [23], Nédélec and Wolf proved the convergence of the homogenization method for linear time-harmonic eddy current problems in a transformer core. In [9, 27], Cao et al studied multi-scale methods for Maxwell's equations in a periodic microstructure. But for eddy current problems, the materials consist of finite number of laminations, coils, and the air surrounding them. They do not construct a periodic structure. Rigorous convergence theory is still lacked in homogenization methods for time-dependent and nonlinear eddy current problems.

The theme of this work is focused on the homogenization of time-dependent eddy current problems in a variational framework. In the engineering community, there are two widely-used formulations of the eddy current model, the $\boldsymbol{H}$-formulation and the $\boldsymbol{A}$-formulation, which are based on the magnetic field and the magnetic vector potential respectively. We start from the micro-scale $\boldsymbol{H}$-formulation to derive the homogenized eddy current model. The main contributions of this paper are as follows:

1. We propose a homogenized $\boldsymbol{H}$-formulation for linear time-dependent eddy current problems. All steel laminations are viewed as a conducting block in the macro-scale problem and the small parameter ϵ is neglected. The model only involves a 3D Laplacian and a 2D Laplacian and can be solved very efficiently by nodal element methods instead of edge element methods.
2. By using weighted norms, we establish the well-posedness of the macro-scale problem. We prove that the micro-scale solutions $\{\boldsymbol{H}_\epsilon\}_{\epsilon>0}$ converge to the macro solution $\boldsymbol{H}_0$ weakly in $\boldsymbol{L}^2(0,T;\boldsymbol{H}(\mathbf{curl},\Omega))$ and strongly in $\boldsymbol{L}^2(0,T;\boldsymbol{L}^2(\Omega))$ as $\epsilon \to 0$.
3. The homogenized Maxwell's equations are derived by choosing proper test functions in the homogenized $\boldsymbol{H}$-formulation. Then the homogenized $\boldsymbol{A}$-formulation is derived easily from the Maxwell's equations.
4. For nonlinear eddy current problems, we propose the homogenized $\boldsymbol{H}$-formulation and prove that the micro-scale solution converges to the homogenized solution as $\epsilon \to 0$. In the nonlinear case, our theories are restricted to thin coating films which have zero thickness but can still prevent eddy

currents from flowing out each lamination. This is reasonable in practical applications since the film thickness is usually about one percent of the lamination thickness (see Fig. 1.2).

5. We extend the homogenization of the $\boldsymbol{H}$-formulation to multiply-connected conductors. It is well-known that the $\boldsymbol{H}$-formulation meets with discontinuous scalar potential in multiply-connected domains. This makes both theoretical analysis and real computations much complicated. Our model has simple form and insures the curl-free property of the reaction magnetic field outside conductors.
6. To validate the homogenized eddy current problem, we compute an engineering benchmark problem — Team Workshop Problem 21^c–M1 from the International Compumag Society by finite element method. The numerical results show good agreements with the experimental data.

The layout of the paper is as follows. In Section 2, we introduce some notation and Sobolev spaces and fix the setting of multiscale eddy current problem. In Section 3, we propose the $\boldsymbol{H}$-formulation and the $\boldsymbol{A}$-formulation of (1.1) and study the limit of micro-scale solutions. In Section 4, we derive the homogenized $\boldsymbol{H}$-formulation, the homogenized $\boldsymbol{A}$-formulation, and the homogenized Maxwell's equations for linear time-dependent eddy current problems. In Section 5, we derive the homogenized $\boldsymbol{H}$-formulation for nonlinear eddy current problems. In Section 6, we propose the homogenized $\boldsymbol{H}$-formulation for multiply-connected conductors. In Section 7, we validate the homogenized $\boldsymbol{H}$-formulation by finite element computations of an engineering benchmark problem—TEAM Workshop Problem 21^c-M1.

Without specification, C denotes the generic constant which is independent of the sensitive quantities, such as the micro-scale parameter ϵ, all through the paper.

2. Preliminaries. Let the truncation domain Ω be a sufficiently large cube which contains all conductors and coils. Let $L^2(\Omega)$ be the usual Hilbert space of square integrable functions equipped with the following inner product and norm:

$$(u,\, v) := \int_\Omega u(\boldsymbol{x})\, v(\boldsymbol{x}) \mathrm{d}\boldsymbol{x} \quad \text{and} \quad \|u\|_{L^2(\Omega)} := (u,\, u)^{1/2}.$$

Define $H^m(\Omega) := \{v \in L^2(\Omega) : D^\xi v \in L^2(\Omega), |\xi| \leq m\}$ where ξ represents non-negative triple index. Let $H_0^1(\Omega)$ be the subspace of $H^1(\Omega)$ whose functions have zero traces on $\partial\Omega$. Throughout the paper we denote vector-valued quantities by boldface notation, such as $\boldsymbol{L}^2(\Omega) := (L^2(\Omega))^3$.

We define the spaces of functions having square integrable curl by

$$\begin{aligned} \boldsymbol{H}(\mathbf{curl}, \Omega) &:= \{\boldsymbol{v} \in \boldsymbol{L}^2(\Omega) \,:\, \mathbf{curl}\, \boldsymbol{v} \in \boldsymbol{L}^2(\Omega)\}, \\ \boldsymbol{H}_0(\mathbf{curl}, \Omega) &:= \{\boldsymbol{v} \in \boldsymbol{H}(\mathbf{curl}, \Omega) \,:\, \boldsymbol{n} \times \boldsymbol{v} = 0 \ \text{ on } \partial\Omega\}, \end{aligned}$$

which are equipped with the following inner product and norm

$$(\boldsymbol{v}, \boldsymbol{w})_{\boldsymbol{H}(\mathbf{curl},\Omega)} := (\boldsymbol{v}, \boldsymbol{w}) + (\mathbf{curl}\, \boldsymbol{v}, \mathbf{curl}\, \boldsymbol{w}), \ \ \|\boldsymbol{v}\|_{\boldsymbol{H}(\mathbf{curl},\Omega)} := \sqrt{(\boldsymbol{v}, \boldsymbol{v})_{\boldsymbol{H}(\mathbf{curl},\Omega)}}\,.$$

Here $\boldsymbol{n}$ denotes the unit outer normal to $\partial\Omega$. We shall also use the spaces of functions having square integrable divergence

$$\begin{aligned} \boldsymbol{H}(\mathrm{div}, \Omega) &:= \{\boldsymbol{v} \in \boldsymbol{L}^2(\Omega) \,:\, \mathrm{div}\, \boldsymbol{v} \in L^2(\Omega)\}, \\ \boldsymbol{H}_0(\mathrm{div}, \Omega) &:= \{\boldsymbol{v} \in \boldsymbol{H}(\mathrm{div}, \Omega) \,:\, \boldsymbol{n} \cdot \boldsymbol{v} = 0 \ \text{ on } \partial\Omega\}. \end{aligned}$$

which are equipped with the following inner product and norm

$$(\boldsymbol{v}, \boldsymbol{w})_{\boldsymbol{H}(\mathrm{div},\Omega)} := (\boldsymbol{v}, \boldsymbol{w}) + (\mathrm{div}\, \boldsymbol{v}, \mathrm{div}\, \boldsymbol{w}), \quad \|\boldsymbol{v}\|_{\boldsymbol{H}(\mathrm{div},\Omega)} := \sqrt{(\boldsymbol{v}, \boldsymbol{v})_{\boldsymbol{H}(\mathrm{div},\Omega)}}\,.$$

This paper is focused on a class of engineering applications where the conducting domain consists of laminated steel sheets, such as magnetic shields and iron cores in a large power transformer. Let Ω_c denote the conducting domain, $\Omega_{nc} := \Omega\backslash\bar{\Omega}_c$ denote the domain without conduction current, Ω_f denote the domain occupied by the coating films surrounding steel laminations, and define $\tilde{\Omega}_c := \Omega_f \cup \bar{\Omega}_c$. Then

$$\Omega_c = \bigcup_{i=1}^{M} \Omega_i \quad \text{and} \quad \Omega_i \cap \Omega_j = \emptyset \quad \text{for} \;\; i \neq j,$$

where Ω_i denotes each steel lamination for $1 \le i \le M$. Let ϵ be the thickness of each coated lamination, ϵ_f be the thickness of the coating film, and $\epsilon_c = \epsilon - 2\epsilon_f$ be the thickness of each steel sheet (see Fig. 1.2). Throughout the paper, we assume that the two factors

$$\theta_c = \frac{\epsilon_c}{\epsilon}, \qquad \theta_f = \frac{2\epsilon_f}{\epsilon} = 1 - \theta_c \tag{2.1}$$

keep fixed as $\epsilon \to 0$. For simplicity, we choose the truncation domain such that

$$\Omega = (-L,\, L)^3, \qquad L = N\epsilon, \qquad N \in \mathbb{Z}.$$

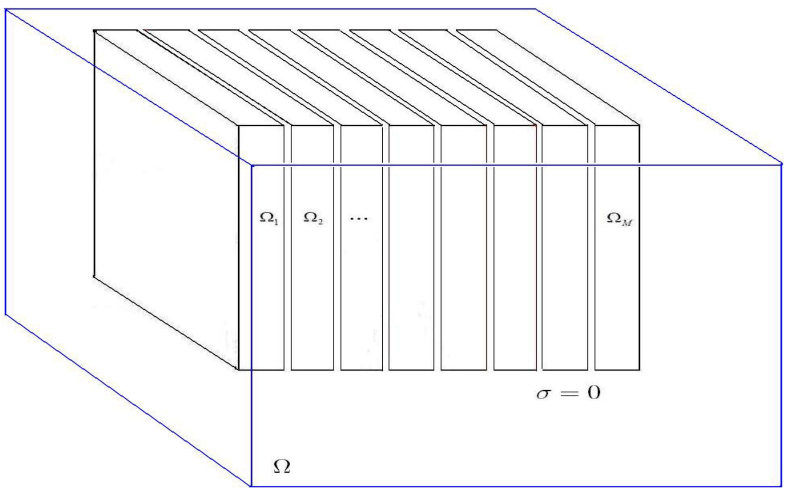

FIG. 2.1. *The truncation domain and the steel laminations.*

The nonlinear relationship between $\boldsymbol{B}$ and $\boldsymbol{H}$ is usually specified by the so-called BH-curves

$$\boldsymbol{B} = \boldsymbol{f}_{\mathrm{BH}}(\boldsymbol{H}). \tag{2.2}$$

In practice, $\boldsymbol{f}_{\mathrm{BH}}$ is usually generated by spline interpolations with experimental data. Figure 2.2 shows the BH-curves in the rolling and transverse directions of GO silicon

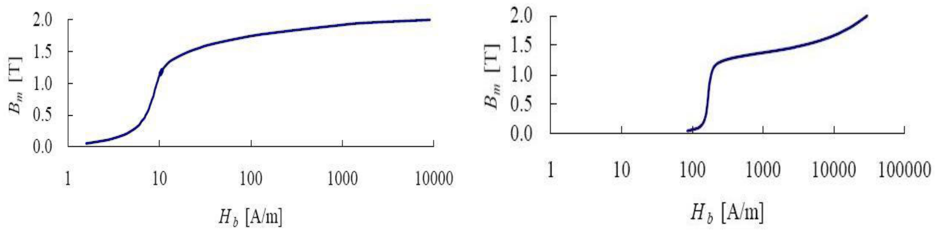

FIG. 2.2. *BH-curves in rolling (left) and transverse (right) directions of silicon steel laminations.*

steel laminations [10]. We assume that the eigenvalues of the Jacobian matrix $\mathbb{J} = \frac{D\boldsymbol{B}}{D\boldsymbol{H}}$ are real and satisfy

$$0 < \mu_{\min} \le \|\lambda_i(\boldsymbol{H})\|_{L^\infty(\mathbb{R}^3)} \le \mu_{\max}, \qquad i = 1, 2, 3. \tag{2.3}$$

Throughout the paper, we append all multi-scale functions with the subscript ϵ, and make the following assumptions on the material parameters and the source current density:

(H1) Let μ_0 be the magnetic permeability in the empty space. The constitutive relation between the flux density and the magnetic field is defined by

$$\boldsymbol{B}_\epsilon(\boldsymbol{H}) = \mu_0 \boldsymbol{H} \quad \text{in } \Omega_{nc}, \qquad \boldsymbol{B}_\epsilon(\boldsymbol{H}) = \boldsymbol{f}_{\mathrm{BH}}(\boldsymbol{H}) \quad \text{in } \Omega_c,$$

(H2) The electric conductivity σ_ϵ is a piecewise constant

$$\sigma_\epsilon \equiv \sigma_0 > 0 \quad \text{in } \Omega_c \qquad \text{and} \qquad \sigma_\epsilon \equiv 0 \quad \text{in } \Omega_{nc}.$$

(H3) The source current density satisfies

$$\boldsymbol{J}_s \in \boldsymbol{L}^2(0, T; \boldsymbol{L}^2(\Omega)), \qquad \boldsymbol{J}(\cdot, 0) = 0, \qquad \operatorname{div} \boldsymbol{J}_s = 0.$$

We remark that the assumptions are rather mild and usually satisfied in electrical engineering.

Denote the truncation boundary by $\Gamma := \partial\Omega$. We impose the initial and boundary conditions for (1.1) and obtain the multi-scale eddy current problem in the bounded domain:

$$\frac{\partial}{\partial t}\boldsymbol{B}_\epsilon(\boldsymbol{H}_\epsilon) + \mathbf{curl}\,\boldsymbol{E}_\epsilon = 0 \quad \text{in } \Omega, \tag{2.4a}$$

$$\mathbf{curl}\,\boldsymbol{H}_\epsilon = \sigma_\epsilon \boldsymbol{E}_\epsilon + \boldsymbol{J}_s \quad \text{in } \Omega, \tag{2.4b}$$

$$\boldsymbol{H}_\epsilon(\cdot, 0) = 0 \quad \text{in } \Omega, \tag{2.4c}$$

$$\boldsymbol{E}_\epsilon \times \boldsymbol{n} = 0 \quad \text{on } \Gamma. \tag{2.4d}$$

3. Weak formulations of the eddy current problem. In this section, we shall study two weak formulations of the eddy current problem which are based on the magnetic field and the magnetic vector potential respectively. The close relationship between the two formulations will play an important role in the homogenization analysis for the eddy current problem. For convenience, we first consider simply-connected laminations, namely, each conductor does not have holes. In this case, we refer to [10] for a family of benchmark problems from the International Compumag Society, such as 21^c-M1, 21^c-M2, 21^c-EM1, 21^c-EM2, and 21^d-M. The theory for multiply-connected conductors will be presented in Section 6.

For simplicity, we assume that the steel sheets are laminated in the x_1-direction and the lamination stack is defined by

$$\tilde{\Omega}_c = \big(0,\ L_1\big) \times \big(0,\ L_2\big) \times \big(0,\ L_3\big),$$

where L_1, L_2, L_3 are fixed as $\epsilon \to 0$. Denote the number of laminations by $M = L_1/\epsilon$. Then the conducting region is defined by

$$\Omega_c = \bigcup_{i=1}^{M} \Omega_i, \qquad \Omega_i = \big(X_i + \epsilon_f,\ X_{i+1} - \epsilon_f\big) \times \big(0,\ L_2\big) \times \big(0,\ L_3\big),$$

where $X_i = (i-1)\epsilon$ for any $1 \le i \le M$. For convenience in notation, we also define

$$\tilde{\Omega}_{nc} = \Omega \backslash \overline{\tilde{\Omega}}_c\ .$$

3.1. The weak $\boldsymbol{H}$-formulation. We first introduce the variational space for the $\boldsymbol{H}$-formulation

$$\mathbf{U}_\epsilon := \nabla H^1(\Omega) + \boldsymbol{H}_0(\mathbf{curl}, \Omega_c). \tag{3.1}$$

Throughout the paper, we shall use the convention that all functions in $\boldsymbol{H}_0(\mathbf{curl}, D)$ and $H_0^1(D)$ are extended by zero to the exterior of D for any $D \subset \Omega$. Then $\mathbf{U}_\epsilon \subset \boldsymbol{H}(\mathbf{curl}, \Omega)$ and

$$\|\boldsymbol{v}\|^2_{\boldsymbol{H}(\mathbf{curl},\Omega)} = \|\boldsymbol{v}\|^2_{\boldsymbol{L}^2(\Omega)} + \|\mathbf{curl}\,\boldsymbol{v}\|^2_{\boldsymbol{L}^2(\Omega_c)} \qquad \forall\, \boldsymbol{v} \in \mathbf{U}_\epsilon.$$

From [22, Theorem 3.1] we know that

$$\mathbf{U}_\epsilon = \{\boldsymbol{v} \in \boldsymbol{H}(\mathbf{curl}, \Omega) :\ \mathbf{curl}\,\boldsymbol{v} = 0 \ \text{ in }\ \Omega_{nc}\}.$$

Lemma 3.1. *[22, Theorem 3.1] For any $\boldsymbol{v} \in \mathbf{U}_\epsilon$, there exist a unique $\phi \in H^1(\Omega)/\mathbb{R}$ and a unique $\boldsymbol{v}_c \in \mathbf{X}_\epsilon := \{\boldsymbol{w} \in \boldsymbol{H}_0(\mathbf{curl}, \Omega_c) :\ \operatorname{div} \boldsymbol{w} = 0\}$ such that*

$$\boldsymbol{v} = \boldsymbol{v}_c + \nabla\phi, \qquad \|\boldsymbol{v}_c\|_{\boldsymbol{H}(\mathbf{curl},\Omega)} + \|\phi\|_{H^1(\Omega)} \le C\, \|\boldsymbol{v}\|_{\boldsymbol{H}(\mathbf{curl},\Omega)}\, ,$$

where the constant $C > 0$ is independent of ϵ.

Since $\operatorname{div} \boldsymbol{J}_s = 0$, we can write $\boldsymbol{J}_s$ into the curl of the source magnetic field by the Biot-Savart Law

$$\boldsymbol{J}_s = \mathbf{curl}\,\boldsymbol{H}_s, \qquad \boldsymbol{H}_s(\boldsymbol{x}) = \frac{1}{4\pi}\,\mathbf{curl} \int_{\mathbb{R}^3} \frac{\boldsymbol{J}_s(\boldsymbol{y})}{|\boldsymbol{x} - \boldsymbol{y}|}\mathrm{d}\boldsymbol{y} \quad \text{in } \mathbb{R}^3. \tag{3.2}$$

In fact we are solving the reaction field $\boldsymbol{R}_\epsilon = \boldsymbol{H}_\epsilon - \boldsymbol{H}_s$. By (2.4b) and (3.2), it satisfies

$$\mathbf{curl}\,\boldsymbol{R}_\epsilon = 0 \quad \text{in }\ \Omega_{nc}.$$

Clearly Lemma 3.1 indicates that $\boldsymbol{R}_\epsilon \in \mathbf{U}_\epsilon$.

For any $\boldsymbol{v} = \nabla\varphi + \boldsymbol{v}_c \in \mathbf{U}_\epsilon$, with $\varphi \in H^1(\Omega)/\mathbb{R}$ and $\boldsymbol{v}_c \in \boldsymbol{H}_0(\mathbf{curl}, \Omega_c)$, from (2.4a)–(2.4b) we have

$$\begin{aligned}\int_\Omega \mathbf{curl}\,\boldsymbol{R}_\epsilon \cdot \mathbf{curl}\,\boldsymbol{v} &= \int_\Omega \sigma_\epsilon \boldsymbol{E}_\epsilon \cdot \mathbf{curl}\,\boldsymbol{v} = \sigma_0 \int_{\Omega_c} \boldsymbol{E}_\epsilon \cdot \mathbf{curl}\,\boldsymbol{v}_c = \sigma_0 \int_\Omega \mathbf{curl}\,\boldsymbol{E}_\epsilon \cdot \boldsymbol{v}_c \\ &= -\sigma_0 \int_\Omega \frac{\partial}{\partial t}\boldsymbol{B}_\epsilon(\boldsymbol{H}_\epsilon) \cdot \boldsymbol{v} - \sigma_0 \int_\Omega \mathbf{curl}\,\boldsymbol{E}_\epsilon \cdot \nabla\varphi.\end{aligned}$$

Using the boundary condition (2.4d), we find that

$$\int_\Omega \mathbf{curl}\, \boldsymbol{E}_\epsilon \cdot \nabla\varphi = -\int_{\partial\Omega} (\boldsymbol{E}_\epsilon \times \boldsymbol{n}) \cdot \nabla\varphi = 0.$$

A weak formulation of (2.4) reads: Find $\boldsymbol{R}_\epsilon \in \boldsymbol{L}^2(0,T;\mathbf{U}_\epsilon)$ such that $\boldsymbol{R}_\epsilon(\cdot,0) = 0$ and

$$\sigma_0 \int_\Omega \frac{\partial}{\partial t} \boldsymbol{B}_\epsilon(\boldsymbol{R}_\epsilon + \boldsymbol{H}_s) \cdot \boldsymbol{v} + \int_\Omega \mathbf{curl}\, \boldsymbol{R}_\epsilon \cdot \mathbf{curl}\, \boldsymbol{v} = 0 \qquad \forall\, \boldsymbol{v} \in \mathbf{U}_\epsilon. \tag{3.3}$$

Here (3.3) is meant in the distributional sense in time.

THEOREM 3.2. *[22, Theorem 3.1] Let (H1)–(H3) be satisfied and suppose* $\boldsymbol{H}_s \in \boldsymbol{H}^1(0,T;\boldsymbol{L}^2(\Omega))$. *Then* (3.3) *has a unique solution* $\boldsymbol{R}_\epsilon \in \boldsymbol{H}^1(0,T;\mathbf{U}_\epsilon)$, *and there exists a constant* C *independent of* ϵ *such that*

$$\|\boldsymbol{R}_\epsilon\|_{\boldsymbol{H}^1(0,T;\boldsymbol{L}^2(\Omega))} + \|\boldsymbol{R}_\epsilon\|_{\boldsymbol{L}^2(0,T;\boldsymbol{H}(\mathbf{curl},\Omega))} \le C\, \|\boldsymbol{H}_s\|_{\boldsymbol{H}^1(0,T;\boldsymbol{L}^2(\Omega))}\,. \tag{3.4}$$

3.2. The weak $\boldsymbol{A}$-formulation. Now we study the $\boldsymbol{A}$-formulation of the eddy current problem. Since $\operatorname{div} \boldsymbol{B}_\epsilon = 0$ by (2.4a) and (2.4c), we can write $\boldsymbol{B}_\epsilon$ into the curl of a magnetic vector potential [19]

$$\boldsymbol{B}_\epsilon = \mathbf{curl}\, \boldsymbol{A}_\epsilon\,, \qquad \boldsymbol{E}_\epsilon = -\frac{\partial \boldsymbol{A}_\epsilon}{\partial t}\,. \tag{3.5}$$

Substituting the above identities into (2.4b) and using (2.4d), we obtain the initial and boundary value problem

$$\sigma_\epsilon \frac{\partial \boldsymbol{A}_\epsilon}{\partial t} + \mathbf{curl}\, \boldsymbol{H}_\epsilon(\mathbf{curl}\, \boldsymbol{A}_\epsilon) = \boldsymbol{J}_s \qquad \text{in } \Omega \times [0,T], \tag{3.6a}$$

$$\boldsymbol{A}_\epsilon \times \boldsymbol{n} = 0 \qquad \text{on } \Gamma \times [0,T], \tag{3.6b}$$

$$\boldsymbol{A}_\epsilon(\cdot,0) = 0 \qquad \text{in } \Omega_c, \tag{3.6c}$$

where $\boldsymbol{H}_\epsilon(\cdot)$ stands for the inverse of the nonlinear function $\boldsymbol{B}_\epsilon(\cdot)$.

A weak formulation of (3.6) reads: Find $\boldsymbol{A}_\epsilon \in \boldsymbol{L}^2(0,T;\boldsymbol{H}_0(\mathbf{curl},\Omega))$ such that $\boldsymbol{A}_\epsilon(\cdot,0) = 0$ and

$$\int_\Omega \sigma_\epsilon \frac{\partial \boldsymbol{A}_\epsilon}{\partial t} \cdot \boldsymbol{v} + \int_\Omega \boldsymbol{H}_\epsilon(\mathbf{curl}\, \boldsymbol{A}_\epsilon) \cdot \mathbf{curl}\, \boldsymbol{v} = \int_\Omega \boldsymbol{J}_s \cdot \boldsymbol{v} \qquad \forall\, \boldsymbol{v} \in \boldsymbol{H}_0(\mathbf{curl},\Omega). \tag{3.7}$$

Here (3.7) is meant in the sense of distributions in time. It is obvious that the solution of (3.7) is not unique in the exterior of Ω_c. In fact, if $\boldsymbol{A}_\epsilon$ solves (3.7), then $\boldsymbol{A}_\epsilon + \xi\nabla p$ also solves (3.7) for any $\xi \in C^1([0,T])$ and

$$p \in H_c^1(\Omega) := \left\{p \in H_0^1(\Omega) :\ p = \text{Const. in } \bar{\Omega}_c\right\}.$$

Clearly $H_c^1(\Omega)$ depends on the small parameter ϵ through Ω_c.

To study the well-posedness of the weak $\boldsymbol{A}$-formulation, we define

$$\boldsymbol{V}_\epsilon = \left\{\boldsymbol{v} \in \boldsymbol{H}_0(\mathbf{curl},\Omega) :\ (\boldsymbol{v},\nabla p) = 0 \quad \forall\, p \in H_c^1(\Omega)\right\}.$$

Let $\boldsymbol{V}_\epsilon$ be endowed with the following inner product and norm

$$(\boldsymbol{v},\boldsymbol{w})_{\boldsymbol{V}_\epsilon} = \int_{\Omega_c} \boldsymbol{v} \cdot \boldsymbol{w} + \int_\Omega \mathbf{curl}\, \boldsymbol{v} \cdot \mathbf{curl}\, \boldsymbol{w}, \qquad \|\boldsymbol{v}\|_{\boldsymbol{V}_\epsilon} = \sqrt{(\boldsymbol{v},\boldsymbol{v})_{\boldsymbol{V}_\epsilon}}\,, \tag{3.8}$$

for any $\boldsymbol{v}, \boldsymbol{w} \in \boldsymbol{V}_\epsilon$. Then we have the orthogonal decomposition

$$\boldsymbol{H}_0(\mathbf{curl}, \Omega) = \boldsymbol{V}_\epsilon \oplus \nabla H^1_{\rm c}(\Omega). \tag{3.9}$$

The following lemma is well-known (cf. e.g. [3, 12, 19]) and plays an important role in the existence and uniqueness of the weak solution.

LEMMA 3.3. *There exists a constant $C_\epsilon > 0$ depending only on Ω_c, Ω such that*

$$\|\boldsymbol{v}\|_{\boldsymbol{H}(\mathbf{curl},\Omega)} \le C_\epsilon \|\boldsymbol{v}\|_{\boldsymbol{V}_\epsilon} \qquad \forall\, \boldsymbol{v} \in \boldsymbol{V}_\epsilon\,.$$

A modified weak problem is: Find $\boldsymbol{a}_\epsilon \in \boldsymbol{L}^2(0,T;\boldsymbol{V}_\epsilon)$ such that $\boldsymbol{a}_\epsilon(\cdot,0) = 0$ and

$$\int_\Omega \sigma_\epsilon \frac{\partial \boldsymbol{a}_\epsilon}{\partial t} \cdot \boldsymbol{v} + \int_\Omega \boldsymbol{H}_\epsilon(\mathbf{curl}\,\boldsymbol{a}_\epsilon) \cdot \mathbf{curl}\,\boldsymbol{v} = \int_\Omega \boldsymbol{J}_s \cdot \boldsymbol{v} \qquad \forall\, \boldsymbol{v} \in \boldsymbol{V}_\epsilon. \tag{3.10}$$

From (3.9), it is easy to see that $\boldsymbol{a}_\epsilon$ also satisfies

$$\int_\Omega \sigma_\epsilon \frac{\partial \boldsymbol{a}_\epsilon}{\partial t} \cdot \boldsymbol{v} + \int_\Omega \boldsymbol{H}_\epsilon(\mathbf{curl}\,\boldsymbol{a}_\epsilon) \cdot \mathbf{curl}\,\boldsymbol{v} = \int_\Omega \boldsymbol{J}_s \cdot \boldsymbol{v} \qquad \forall\, \boldsymbol{v} \in \boldsymbol{H}_0(\mathbf{curl}, \Omega). \tag{3.11}$$

This means that $\boldsymbol{a}_\epsilon$ is one solution of (3.7). Here (3.10) and (3.11) are also meant in the distributional sense in time. Although the solution of (3.7) is not unique, the current density and the magnetic flux density are unique, namely,

$$\frac{\partial}{\partial t}(\sigma_\epsilon \boldsymbol{A}_\epsilon) = \frac{\partial}{\partial t}(\sigma_\epsilon \boldsymbol{a}_\epsilon), \qquad \mathbf{curl}\,\boldsymbol{A}_\epsilon = \mathbf{curl}\,\boldsymbol{a}_\epsilon \qquad \text{in } \ \Omega. \tag{3.12}$$

Therefore, we are only interested in $\sigma_\epsilon \boldsymbol{a}_\epsilon$ and $\mathbf{curl}\,\boldsymbol{a}_\epsilon$ throughout this paper.

THEOREM 3.4. *([19, Theorem 2.2]) Let (H1)–(H3) be satisfied. Then* (3.10) *has a unique solution and there exists a constant $C > 0$ independent of ϵ such that*

$$\|\sigma_\epsilon \boldsymbol{a}_\epsilon\|_{\boldsymbol{L}^2(0,T;\boldsymbol{L}^2(\Omega))} + \|\mathbf{curl}\,\boldsymbol{a}_\epsilon\|_{\boldsymbol{L}^2(0,T;\boldsymbol{L}^2(\Omega))} \le C \|\boldsymbol{J}_s\|_{\boldsymbol{L}^2(0,T;\boldsymbol{L}^2(\Omega))}\,. \tag{3.13}$$

3.3. Weak limit of the micro-scale solutions. Now we are going to study the limit of the micro-scale solutions as the thickness of steel lamination tends to zero.

Let $\boldsymbol{R}_\epsilon$ be the solution of (3.3). From Theorem 3.2, there exists a subsequence of $\{\boldsymbol{R}_\epsilon\}_{\epsilon>0}$ such that

$$\lim_{\epsilon \to 0} \boldsymbol{R}_\epsilon = \boldsymbol{R}_0 \qquad \text{weakly in } \ \boldsymbol{L}^2(0,T;\boldsymbol{H}(\mathbf{curl},\Omega)). \tag{3.14}$$

Since $\boldsymbol{H}_s$ is smooth, it follows that

$$\lim_{\epsilon \to 0} \boldsymbol{H}_\epsilon = \boldsymbol{H}_0 := \boldsymbol{R}_0 + \boldsymbol{H}_s \qquad \text{weakly in } \ \boldsymbol{L}^2(0,T;\boldsymbol{H}(\mathbf{curl},\Omega)). \tag{3.15}$$

By Lemma 3.1, the reaction field $\boldsymbol{R}_\epsilon$ admits a unique decomposition

$$\boldsymbol{R}_\epsilon = \boldsymbol{u}_\epsilon + \nabla \psi_\epsilon, \qquad \|\boldsymbol{u}_\epsilon\|_{\boldsymbol{H}(\mathbf{curl},\Omega)} + \|\psi_\epsilon\|_{H^1(\Omega)} \le C \|\boldsymbol{R}_\epsilon\|_{\boldsymbol{H}(\mathbf{curl},\Omega)}\,, \tag{3.16}$$

where $\boldsymbol{u}_\epsilon \in \boldsymbol{X}_\epsilon$, $\psi_\epsilon \in H^1(\Omega)/\mathbb{R}$, and the constant C is independent of ϵ. From (3.4) and (3.16) we know that, with a constant C independent of ϵ,

$$\|\boldsymbol{u}_\epsilon\|_{\boldsymbol{H}^1(0,T;\boldsymbol{L}^2(\Omega))} + \|\boldsymbol{u}_\epsilon\|_{\boldsymbol{L}^2(0,T;\boldsymbol{H}(\mathbf{curl},\Omega))} + \|\psi_\epsilon\|_{H^1(0,T;H^1(\Omega))} \le C. \tag{3.17}$$

Since $\boldsymbol{L}^2(0,T;\boldsymbol{H}(\mathbf{curl},\Omega))$ and $H^1(0,T;H^1(\Omega))$ are self-reflective, there are two subsequences still denoted by $\{\boldsymbol{u}_\epsilon\}_{\epsilon>0}$ and $\{\psi_\epsilon\}_{\epsilon>0}$ such that

$$\lim_{\epsilon\to 0}\boldsymbol{u}_\epsilon=\boldsymbol{u}_0 \qquad \text{weakly in } \boldsymbol{L}^2(0,T;\boldsymbol{H}(\mathbf{curl},\Omega)), \tag{3.18}$$

$$\lim_{\epsilon\to 0}\psi_\epsilon=\psi_0 \qquad \text{weakly in } H^1(0,T;H^1(\Omega)). \tag{3.19}$$

Clearly we have

$$\boldsymbol{R}_0=\boldsymbol{u}_0+\nabla\psi_0. \tag{3.20}$$

Now we are going to show that $\boldsymbol{u}_0$ only has one nonzero component. Let S_c, S_i denote the parts of $\partial\tilde{\Omega}_c$ and $\partial\Omega_i$ respectively whose unit normals are parallel to $\boldsymbol{e}_1=(1,0,0)$, namely,

$$S_c=\left\{\boldsymbol{x}\in\partial\tilde{\Omega}_c:\ \boldsymbol{n}_{\boldsymbol{x}}\parallel\boldsymbol{e}_1\right\},\quad S_i=\left\{\boldsymbol{x}\in\partial\Omega_i:\ \boldsymbol{n}_{\boldsymbol{x}}\parallel\boldsymbol{e}_1\right\},\quad 1\le i\le M.$$

We introduce the following Hilbert spaces

$$\mathcal{H}^1(\tilde{\Omega}_c)=\left\{v\in L^2(\tilde{\Omega}_c):\ \frac{\partial v}{\partial x_2},\frac{\partial v}{\partial x_3}\in L^2(\tilde{\Omega}_c)\right\},$$
$$\mathcal{H}^1_0(\tilde{\Omega}_c)=\left\{v\in\mathcal{H}^1(\tilde{\Omega}_c):\ v=0\ \text{ on } \partial\tilde{\Omega}_c\backslash\bar{S}_c\right\},$$

which are equipped with the inner product and norm

$$(u,v)_{\mathcal{H}^1(\tilde{\Omega}_c)}=\int_{\tilde{\Omega}_c}\left(uv+\frac{\partial u}{\partial x_2}\frac{\partial v}{\partial x_2}+\frac{\partial u}{\partial x_3}\frac{\partial v}{\partial x_3}\right),\quad \|v\|_{\mathcal{H}^1(\tilde{\Omega}_c)}=(v,v)^{1/2}_{\mathcal{H}^1(\tilde{\Omega}_c)}.$$

LEMMA 3.5. *Let $\boldsymbol{u}_0$ be the limit of $\{\boldsymbol{u}_\epsilon\}_\epsilon$. Then $\boldsymbol{u}_0=u\,\boldsymbol{e}_1$ where $u\in\mathcal{H}^1_0(\tilde{\Omega}_c)$.*

Proof. Since $\boldsymbol{u}_\epsilon\in\boldsymbol{H}_0(\mathbf{curl},\tilde{\Omega}_c)$, we also have $\boldsymbol{u}_0\in\boldsymbol{H}_0(\mathbf{curl},\tilde{\Omega}_c)$. Write $\boldsymbol{u}_\epsilon=(u_{\epsilon,1},u_{\epsilon,2},u_{\epsilon,3})$ and $\boldsymbol{u}_0=(u_1,u_2,u_3)$. If $u_2=u_3=0$, then

$$\mathbf{curl}\,\boldsymbol{u}_0=\left(0,\ \frac{\partial u_1}{\partial x_3},\ -\frac{\partial u_1}{\partial x_2}\right)\in\boldsymbol{L}^2(\tilde{\Omega}_c),\quad |\boldsymbol{u}_0\times\boldsymbol{n}|=|u_1|=0\quad\text{on } \partial\tilde{\Omega}_c\backslash\bar{S}_c.$$

This shows that $u_1\in\mathcal{H}^1_0(\tilde{\Omega}_c)$. It is left to prove $u_2=u_3=0$.

From Lemma 3.1, it is easy to see $\boldsymbol{u}_\epsilon\in\boldsymbol{X}_\epsilon$. Since Ω_i is convex, the embedding theorem in [2] shows that $\boldsymbol{u}_\epsilon\in\boldsymbol{H}^1(\Omega_i)$ for any $1\le i\le M$. The boundary condition $\boldsymbol{u}_\epsilon\times\boldsymbol{n}=0$ on S_i indicates that

$$u_{\epsilon,2}=u_{\epsilon,3}=0\quad\text{on}\ S_i,\qquad u_{\epsilon,1}=0\quad\text{on}\ \partial\Omega_i\backslash\bar{S}_i. \tag{3.21}$$

For any $\varphi\in C_0^\infty(\tilde{\Omega}_c)$, (3.21) shows that $u_{\epsilon,2}(X_i+\epsilon_f,\cdot,\cdot)\equiv 0$. Then

$$\int_{\Omega_i}\varphi(\boldsymbol{x})u_{\epsilon,2}(\boldsymbol{x})\mathrm{d}\boldsymbol{x}=\int_{\Omega_i}\varphi(\boldsymbol{x})\int_{X_i+\epsilon_f}^{x_1}\frac{\partial u_{\epsilon,2}}{\partial y}(y,x_2,x_3)\mathrm{d}y\mathrm{d}\boldsymbol{x}=G_{i,1}+G_{i,2}, \tag{3.22}$$

where

$$G_{i,1}=\int_{\Omega_i}\int_{X_i+\epsilon_f}^{x_1}\varphi(\boldsymbol{x})\left[\frac{\partial u_{\epsilon,2}}{\partial y}(y,x_2,x_3)-\frac{\partial u_{\epsilon,1}}{\partial x_2}(y,x_2,x_3)\right]\mathrm{d}y\mathrm{d}\boldsymbol{x},$$
$$G_{i,2}=\int_{\Omega_i}\int_{X_i+\epsilon_f}^{x_1}\varphi(\boldsymbol{x})\frac{\partial u_{\epsilon,1}}{\partial x_2}(y,x_2,x_3)\mathrm{d}y\mathrm{d}\boldsymbol{x}.$$

An application of Schwarz's inequality yields

$$|G_{i,1}| \le \int_{\Omega_i} |\varphi| \int_{X_i+\epsilon_f}^{X_{i+1}-\epsilon_f} |\mathbf{curl}\, \boldsymbol{u}_\epsilon(y,\cdot,\cdot)|\, \mathrm{d}y \le \epsilon \, \|\varphi\|_{L^2(\Omega_i)} \, \|\mathbf{curl}\, \boldsymbol{u}_\epsilon\|_{\boldsymbol{L}^2(\Omega_i)} \, .$$

By (3.21) and the formula of integral by part, the second term is estimated as follows

$$\begin{aligned}|G_{2,i}| =& \left| \int_{\Omega_i} \varphi \cdot \frac{\partial}{\partial x_2} \int_{X_i+\epsilon_f}^{x_1} u_{\epsilon,1}(y,\cdot,\cdot)\mathrm{d}y \right| = \left| \int_{\Omega_i} \frac{\partial \varphi}{\partial x_2} \cdot \int_{X_i+\epsilon_f}^{x_1} u_{\epsilon,1}(y,\cdot,\cdot)\mathrm{d}y \right| \\ \le& \epsilon |\varphi|_{H^1(\Omega_i)} \, \|u_{\epsilon,1}\|_{L^2(\Omega_i)} \, .\end{aligned}$$

Substituting the estimates for $G_{i,1}$ and $G_{i,2}$ into (3.22) and summing up the estimates in $1 \le i \le M$, we get

$$\left| \int_{\tilde{\Omega}_c} \varphi u_{\epsilon,2} \right| \le C\epsilon \|\varphi\|_{H^1(\tilde{\Omega}_c)} \, \|\boldsymbol{u}_\epsilon\|_{\boldsymbol{H}(\mathbf{curl},\tilde{\Omega}_c)} \, .$$

In view of (3.17), the above inequality shows that

$$\left| \int_0^T \int_{\tilde{\Omega}_c} \varphi u_{\epsilon,2} \right| \le C\epsilon \, \|\varphi\|_{L^2(0,T;H^1(\tilde{\Omega}_c))} \, \|\boldsymbol{u}_\epsilon\|_{\boldsymbol{L}^2(0,T;\boldsymbol{H}(\mathbf{curl},\tilde{\Omega}_c))} \le C\epsilon.$$

where the constant C is independent of ϵ. This means that

$$\int_0^T \int_{\tilde{\Omega}_c} \varphi u_2 = \lim_{\epsilon \to 0} \int_0^T \int_{\tilde{\Omega}_c} \varphi u_{\epsilon,2} = 0 \qquad \forall\, \varphi \in L^2(0,T;C_0^\infty(\tilde{\Omega}_c)).$$

Hence we have $u_2 = 0$. The proof for $u_3 = 0$ is similar and omitted here. □

Now Lemma 3.5 shows that $\boldsymbol{R}_0 = u\, \boldsymbol{e}_1 + \nabla \psi_0 \in \boldsymbol{X}_0$, where

$$\boldsymbol{X}_0 := \mathcal{H}_0^1(\tilde{\Omega}_c)\, \boldsymbol{e}_1 + \nabla H^1(\Omega). \tag{3.23}$$

LEMMA 3.6. *Let $\boldsymbol{R}_0$ be the weak limit of $\boldsymbol{R}_\epsilon$ in $\boldsymbol{L}^2(0,T;\boldsymbol{H}(\mathbf{curl},\Omega))$. Then*

$$\boldsymbol{R}_0(\cdot,0) = 0 \quad \textit{in} \ \ \Omega.$$

Proof. From (3.4), it is easy to prove that

$$\lim_{\epsilon \to 0} \boldsymbol{R}_\epsilon = \boldsymbol{R}_0 \qquad \text{also weakly in } \ \boldsymbol{H}^1(0,T;\boldsymbol{L}^2(\Omega)).$$

Take any $\varphi \in C^\infty([0,T])$ satisfying $\varphi(0) = 1$ and $\varphi(T) = 0$. Then the formula of integration by parts shows that, for any $\boldsymbol{v} \in \boldsymbol{L}^2(\Omega)$,

$$\begin{aligned}(\boldsymbol{R}_0(\cdot,0),\boldsymbol{v}) =& \int_0^T \left\{ \varphi(t) \cdot \frac{\partial}{\partial t}(\boldsymbol{R}_0,\boldsymbol{v}) + \varphi'(t) \cdot (\boldsymbol{R}_0,\boldsymbol{v}) \right\} \mathrm{d}t \\ =& \lim_{\epsilon \to 0} \int_0^T \left\{ \varphi(t) \cdot \frac{\partial}{\partial t}(\boldsymbol{R}_\epsilon,\boldsymbol{v}) + \varphi'(t) \cdot (\boldsymbol{R}_\epsilon,\boldsymbol{v}) \right\} \mathrm{d}t = \lim_{\epsilon \to 0}(\boldsymbol{R}_\epsilon(\cdot,0),\boldsymbol{v}).\end{aligned}$$

The proof is completed upon using the initial condition $\boldsymbol{R}_\epsilon(\cdot,0) = 0$. □

From Theorem 3.2 and (2.3), there exists a constant C independent of ϵ such that

$$\|\boldsymbol{B}_\epsilon(\boldsymbol{H}_\epsilon)\|_{\boldsymbol{L}^2(0,T;\boldsymbol{L}^2(\Omega))} + \|\mathbf{curl}\,\boldsymbol{R}_\epsilon\|_{\boldsymbol{L}^2(0,T;\boldsymbol{L}^2(\tilde{\Omega}_c))} \le C.$$

Then there is a common subsequence of $\{\boldsymbol{B}_\epsilon(\boldsymbol{H}_\epsilon)\}_{\epsilon>0}$ and $\{\mathbf{curl}\,\boldsymbol{R}_\epsilon\}_{\epsilon>0}$ still denoted by the same notation such that

$$\lim_{\epsilon\to 0} \boldsymbol{B}_\epsilon(\boldsymbol{H}_\epsilon) = \boldsymbol{B}_0 \qquad \text{weakly in } \boldsymbol{L}^2(0,T;\boldsymbol{L}^2(\Omega)), \tag{3.24}$$

$$\lim_{\epsilon\to 0} \mathbf{curl}\,\boldsymbol{R}_\epsilon = \boldsymbol{J}_0 \qquad \text{weakly in } \boldsymbol{L}^2(0,T;\boldsymbol{L}^2(\tilde{\Omega}_c)). \tag{3.25}$$

The following lemma is a direct consequence of Lemma 3.5, (3.18), and (3.25).

LEMMA 3.7. *Let* $\boldsymbol{u}_0 = u\,\boldsymbol{e}_1$ *be the limit of* $\{\boldsymbol{u}_\epsilon\}_{\epsilon>0}$ *in* (3.18). *Then*

$$\boldsymbol{J}_0 = \mathbf{curl}\,\boldsymbol{u}_0 = \mathbf{curl}(u\boldsymbol{e}_1) \quad \text{in } \tilde{\Omega}_c.$$

REMARK 3.8. *From Lemma 3.7, it is easy to see that the first component of the homogenized eddy current density is zero. By macro-scale models, we can not compute eddy currents flowing in the normal direction to the lamination plane.*

4. Homogenization of linear eddy current problem.

The purpose of this section is to derive the homogenized eddy current problem for nonmagnetic materials. In this case, we have $\boldsymbol{B}(\boldsymbol{H}) = \mu_0 \boldsymbol{H}$ in Ω. For simplicity, we neglect the eddy current density in coils and assume

$$\operatorname{supp}(\boldsymbol{J}_s) \cap \tilde{\Omega}_c = \emptyset.$$

4.1. The homogenized $\boldsymbol{H}$-formulation.

We start by presenting the strong convergence of the micro-scale solutions in $\boldsymbol{L}^2(0,T;\boldsymbol{L}^2(\Omega))$.

LEMMA 4.1. *Let* $\boldsymbol{R}_\epsilon$ *be the solution of* (3.3) *and* $\boldsymbol{R}_0$ *be the weak limit of* $\boldsymbol{R}_\epsilon$ *in* (3.14). *Then*

$$\lim_{\epsilon\to 0} \|\boldsymbol{R}_\epsilon - \boldsymbol{R}_0\|_{\boldsymbol{L}^2(0,T;\boldsymbol{L}^2(\Omega))} = 0. \tag{4.1}$$

Proof. The proof is similar to Lemma 5.1 for nonlinear case and omitted here. ∎

To derive the macro-scale model, we introduce the characteristic function χ_ϵ defined as follows

$$\chi_\epsilon = \begin{cases} 1 & \text{in } \Omega_c\,, \\ 0 & \text{elsewhere}\,. \end{cases} \tag{4.2}$$

It is known that $\lim_{\epsilon\to 0}\chi_\epsilon = \theta_c$ weakly star in $L^\infty(\tilde{\Omega}_c)$, namely

$$\lim_{\epsilon\to 0} \int_{\tilde{\Omega}_c} \chi_\epsilon v = \int_{\tilde{\Omega}_c} \theta_c v \qquad \forall\, v \in L^1(\tilde{\Omega}_c)\,. \tag{4.3}$$

LEMMA 4.2. *Let* $\boldsymbol{v}_\epsilon = \chi_\epsilon v \boldsymbol{e}_1$ *where* $v \in \mathcal{H}_0^1(\tilde{\Omega}_c)$. *Then* $\boldsymbol{v}_\epsilon \in \boldsymbol{H}_0(\mathbf{curl}, \Omega_c)$.

Proof. For any fixed $v \in \mathcal{H}_0^1(\tilde{\Omega}_c)$, we have

$$\boldsymbol{v}_\epsilon \times \boldsymbol{e}_1 = 0 \quad \text{on } \cup_{i=1}^I S_i,$$
$$|\boldsymbol{v}_\epsilon \times \boldsymbol{e}_2| = |\boldsymbol{v}_\epsilon \times \boldsymbol{e}_3| = |v_1| = 0 \quad \text{on } \partial\tilde{\Omega}_c \backslash \bar{S}_c.$$

This means that $\boldsymbol{v}_\epsilon \times \boldsymbol{n} = 0$ on $\partial\Omega_c$. Moreover, the definition of $\mathcal{H}_0^1(\tilde{\Omega}_c)$ indicates that

$$\|\boldsymbol{v}_\epsilon\|_{\boldsymbol{L}^2(\Omega_c)} = \|v\|_{L^2(\Omega_c)} < \infty,$$
$$\|\mathbf{curl}\,\boldsymbol{v}_\epsilon\|_{\boldsymbol{L}^2(\Omega_c)} = \left(\left\| \frac{\partial v}{\partial x_2} \right\|^2_{L^2(\Omega_c)} + \left\| \frac{\partial v}{\partial x_3} \right\|^2_{L^2(\Omega_c)} \right)^{1/2} < \infty.$$

Thus we conclude that $\boldsymbol{v}_\epsilon \in \boldsymbol{H}_0(\mathbf{curl}, \Omega_c)$. □

THEOREM 4.3. *Let $\boldsymbol{R}_\epsilon$ be the solution of* (3.3) *and let $\boldsymbol{R}_0 = \nabla\psi_0 + u\boldsymbol{e}_1$ be the limit of $\boldsymbol{R}_\epsilon$. Then $\boldsymbol{R}_0$ solves the following macro-scale problem: Find $\boldsymbol{R}_0 \in \boldsymbol{L}^2(0,T;\boldsymbol{X}_0)$ such that $\boldsymbol{R}_0(\cdot,0) = 0$ and*

$$\theta_c\sigma_0\mu_0 \int_\Omega \frac{\partial}{\partial t}(\boldsymbol{R}_0 + \boldsymbol{H}_s)\cdot\boldsymbol{v} + \int_\Omega \mathbf{curl}\,\boldsymbol{R}_0 \cdot \mathbf{curl}\,\boldsymbol{v} = 0 \qquad \forall\, \boldsymbol{v} \in \boldsymbol{X}_0. \tag{4.4}$$

Proof. Noting that $\boldsymbol{B} = \mu_0\boldsymbol{H}$ in Ω, the weak formulation (3.3) is equivalent to

$$\sigma_0\mu_0 \int_0^T \int_\Omega \frac{\partial}{\partial t}(\boldsymbol{R}_\epsilon + \boldsymbol{H}_s)\cdot\boldsymbol{v}_\epsilon + \int_0^T \int_\Omega \mathbf{curl}\,\boldsymbol{R}_\epsilon \cdot \mathbf{curl}\,\boldsymbol{v}_\epsilon = 0 \;\; \forall\, \boldsymbol{v}_\epsilon \in \boldsymbol{C}_0^\infty(0,T;\mathbf{U}_\epsilon).$$

From Lemma 4.2, we know that the above equality holds for all $\boldsymbol{v}_\epsilon = \chi_\epsilon v\boldsymbol{e}_1$, $v \in C_0^\infty(0,T;\mathcal{H}_0^1(\tilde{\Omega}_c))$. Then

$$\sigma_0\mu_0 \int_0^T \int_\Omega \frac{\partial}{\partial t}(\boldsymbol{R}_\epsilon + \boldsymbol{H}_s)\cdot(\chi_\epsilon v\boldsymbol{e}_1) + \int_0^T \int_\Omega \mathbf{curl}\,\boldsymbol{R}_\epsilon \cdot \mathbf{curl}(\chi_\epsilon v\boldsymbol{e}_1) = 0,$$

Since $\mathrm{supp}(\mathbf{curl}\,\boldsymbol{R}_\epsilon) = \mathrm{supp}(\mathbf{curl}\,\boldsymbol{u}_\epsilon) \subset \bar{\Omega}_c$, we have

$$-\sigma_0\mu_0 \int_0^T \int_\Omega [(\boldsymbol{R}_\epsilon + \boldsymbol{H}_s)\cdot\boldsymbol{e}_1]\,\chi_\epsilon \frac{\partial v}{\partial t} + \int_0^T \int_\Omega \mathbf{curl}\,\boldsymbol{R}_\epsilon \cdot \mathbf{curl}(v\boldsymbol{e}_1) = 0.$$

Using Lemma 4.1 and (4.3) and letting ϵ tend to zero, the above equality yields that, for any $v \in C_0^\infty(0,T;\mathcal{H}_0^1(\tilde{\Omega}_c))$,

$$-\theta_c\sigma_0\mu_0 \int_0^T \int_\Omega [(\boldsymbol{R}_0 + \boldsymbol{H}_s)\cdot\boldsymbol{e}_1]\,\frac{\partial v}{\partial t} + \int_0^T \int_\Omega \mathbf{curl}\,\boldsymbol{R}_0 \cdot \mathbf{curl}(v\boldsymbol{e}_1) = 0,$$

or equivalently,

$$\theta_c\sigma_0\mu_0 \int_0^T \int_\Omega \frac{\partial}{\partial t}(\boldsymbol{R}_0 + \boldsymbol{H}_s)\cdot(v\boldsymbol{e}_1) + \int_0^T \int_\Omega \mathbf{curl}\,\boldsymbol{R}_0 \cdot \mathbf{curl}(v\boldsymbol{e}_1) = 0.$$

Moreover, for any $\varphi \in C_0^\infty(0,T;H^1(\Omega))$, from (3.24) we know that

$$\int_0^T \int_\Omega \mu_0 \frac{\partial}{\partial t}(\boldsymbol{R}_0 + \boldsymbol{H}_s)\cdot\nabla\varphi = \int_0^T \int_\Omega \frac{\partial \boldsymbol{B}_0}{\partial t}\cdot\nabla\varphi = \lim_{\epsilon\to 0} \int_0^T \int_\Omega \frac{\partial}{\partial t}\boldsymbol{B}_\epsilon(\boldsymbol{H}_\epsilon)\cdot\nabla\varphi = 0.$$

Combining the above two equalities, $\boldsymbol{R}_0$ satisfies (4.4) in a distributional sense. □

THEOREM 4.4. *The homogenized problem* (4.4) *has a unique solution. And there is a constant C independent of ϵ such that*

$$\|\boldsymbol{R}_0\|_{\boldsymbol{L}^\infty(0,T;\boldsymbol{L}^2(\Omega))} + \|\mathbf{curl}\,\boldsymbol{R}_0\|_{\boldsymbol{L}^2(0,T;\boldsymbol{L}^2(\Omega))} \le C\,\|\boldsymbol{H}_s\|_{\boldsymbol{H}^1(0,T;\boldsymbol{L}^2(\Omega))}\,.$$

Proof. In fact, Theorem 4.3 shows that $\boldsymbol{R}_0$ is one solution of (4.4). It is left to prove the uniqueness. The stability can be proved by standard arguments for parabolic problems and is omitted for simplicity. The uniqueness follows directly from the stability estimate. ☐

REMARK 4.5. *Notice that*

$$\mathbf{curl}\,\boldsymbol{R}_0 = \mathbf{curl}(u\boldsymbol{e}_1) = \left(0,\, \frac{\partial u}{\partial x_3},\, -\frac{\partial u}{\partial x_2}\right).$$

Problem (4.4) *can be rewritten as: Find* $\psi_0 \in H^1(\Omega)/\mathbb{R}$ *and* $u \in \mathcal{H}_0^1(\tilde{\Omega}_c)$ *such that* $\psi_0(\cdot,0) = 0$, $u(\cdot,0) = 0$, *and*

$$\int_\Omega \frac{\partial}{\partial t}(\nabla\psi_0 + u\boldsymbol{e}_1) \,\cdot\, (\nabla\varphi + v\boldsymbol{e}_1) + \frac{1}{\theta_c\sigma_0\mu_0}\int_{\tilde{\Omega}_c}\left(\frac{\partial u}{\partial x_2}\frac{\partial v}{\partial x_2} + \frac{\partial u}{\partial x_3}\frac{\partial v}{\partial x_3}\right) \tag{4.5}$$
$$= -\int_\Omega \frac{\partial \boldsymbol{H}_s}{\partial t}\cdot(\nabla\varphi + v\boldsymbol{e}_1) \qquad \forall\,\varphi \in H^1(\Omega),\ \ v \in \mathcal{H}_0^1(\tilde{\Omega}_c).$$

Clearly (4.5) *only involves a 3D Laplacian for* ψ *in* Ω *and a 2D Laplacian for* u *in* $\tilde{\Omega}_c$. *It can be solved by nodal finite element method instead of edge element method. This simplifies the computations greatly. We shall validate* (4.5) *numerically in Section 7.*

4.2. The homogenized Maxwell's equations. From (3.3), it is easy to see that

$$\int_\Omega \boldsymbol{B}_0\cdot\nabla\phi = \lim_{\epsilon\to 0}\int_\Omega \boldsymbol{B}_\epsilon\cdot\nabla\phi = 0 \qquad \forall\,\phi \in H^1(\Omega),$$

which implies that

$$\operatorname{div}\boldsymbol{B}_0 = 0 \quad \text{in}\ \ \Omega \qquad \text{and} \qquad \boldsymbol{B}_0\cdot\boldsymbol{n} = 0 \quad \text{on}\ \ \Gamma.$$

Then there exists a unique potential $\boldsymbol{A}_0 \in \boldsymbol{H}_0(\mathbf{curl},\Omega)$ such that

$$\boldsymbol{B}_0 = \mathbf{curl}\,\boldsymbol{A}_0, \quad \operatorname{div}\boldsymbol{A}_0 = 0 \quad \text{in}\ \ \Omega\,. \tag{4.6}$$

We define the homogenized electric field by

$$\boldsymbol{E}_0 := -\frac{\partial \boldsymbol{A}_0}{\partial t}. \tag{4.7}$$

To derive the homogenized Maxwell's equations for $\boldsymbol{E}_0$ and $\boldsymbol{H}_0$, we first introduce the following lemma.

LEMMA 4.6. *Let* θ_c *be the effective factor in* (2.1). *Then*

$$\theta_c\sigma_0\int_{\tilde{\Omega}_c}\frac{\partial \boldsymbol{B}_0}{\partial t}\cdot\boldsymbol{v} + \int_{\tilde{\Omega}_c}\mathbf{curl}\,\boldsymbol{H}_0\cdot\mathbf{curl}\,\boldsymbol{v} = 0 \qquad \forall\,\boldsymbol{v}\in \boldsymbol{C}_0^\infty(\tilde{\Omega}_c). \tag{4.8}$$

Proof. For any $v \in C_0^\infty(\tilde{\Omega}_c)$ satisfying $\operatorname{div}(v\boldsymbol{e}_2) = 0$, we have

$$\int_{\tilde{\Omega}_c}\boldsymbol{B}_0\cdot(v\boldsymbol{e}_2) = \mu_0\int_{\tilde{\Omega}_c}(u\boldsymbol{e}_1 + \nabla\psi_0 + \boldsymbol{H}_s)\cdot(v\boldsymbol{e}_2) = \mu_0\int_{\tilde{\Omega}_c}\boldsymbol{H}_s\cdot(v\boldsymbol{e}_2).$$

Since $\tilde{\Omega}_c$ is simply-connected, there exist a $\mathbf{\Phi} \in \boldsymbol{H}_0(\mathbf{curl}, \tilde{\Omega}_c)$ and a $\phi \in H_0^1(\tilde{\Omega}_c)$ such that (cf. e.g. [2])

$$v\boldsymbol{e}_2 = \mathbf{curl}\,\mathbf{\Phi} + \nabla\phi\,.$$

Since $\operatorname{supp}(\boldsymbol{J}_s) \cap \tilde{\Omega}_c = \emptyset$, (3.2) and the formula of integration by parts show that

$$\int_{\tilde{\Omega}_c} \boldsymbol{B}_0 \cdot (v\boldsymbol{e}_2) = \mu_0 \int_{\tilde{\Omega}_c} \boldsymbol{H}_s \cdot (v\boldsymbol{e}_2) = \mu_0 \int_{\tilde{\Omega}_c} (\mathbf{curl}\,\boldsymbol{H}_s \cdot \mathbf{\Phi} - \operatorname{div} \boldsymbol{H}_s \cdot \phi) = 0.$$

It follows that

$$\int_{\tilde{\Omega}_c} \frac{\partial \boldsymbol{B}_0}{\partial t} \cdot (v\boldsymbol{e}_2) = 0.$$

Noting that $\dfrac{\partial v}{\partial x_2} = \operatorname{div}(v\boldsymbol{e}_2) = 0$, thus

$$\begin{aligned}\int_{\tilde{\Omega}_c} \mathbf{curl}\,\boldsymbol{H}_0 \cdot \mathbf{curl}(v\boldsymbol{e}_2) &= \int_{\tilde{\Omega}_c} \mathbf{curl}(u\boldsymbol{e}_1) \cdot \mathbf{curl}(v\boldsymbol{e}_2) = -\int_{\tilde{\Omega}_c} \frac{\partial u}{\partial x_2}\frac{\partial v}{\partial x_1} \\ &= \int_{\tilde{\Omega}_c} u \frac{\partial^2 v}{\partial x_1 \partial x_2} = 0.\end{aligned}$$

Then we conclude that, for any $v \in C_0^\infty(\tilde{\Omega}_c)$ satisfying $\operatorname{div}(v\boldsymbol{e}_2) = 0$,

$$\theta_c\sigma_0 \int_{\tilde{\Omega}_c} \frac{\partial \boldsymbol{B}_0}{\partial t} \cdot (v\boldsymbol{e}_2) + \int_{\tilde{\Omega}_c} \mathbf{curl}\,\boldsymbol{H}_0 \cdot \mathbf{curl}(v\boldsymbol{e}_2) = 0.$$

From $\operatorname{div} \boldsymbol{B}_0 = 0$, we also deduce that

$$\theta_c\sigma_0 \int_{\tilde{\Omega}_c} \frac{\partial \boldsymbol{B}_0}{\partial t} \cdot (v\boldsymbol{e}_2) + \int_{\tilde{\Omega}_c} \mathbf{curl}\,\boldsymbol{H}_0 \cdot \mathbf{curl}(v\boldsymbol{e}_2) = 0 \qquad \forall\, v \in C_0^\infty(\tilde{\Omega}_c). \tag{4.9}$$

Similarly we have

$$\theta_c\sigma_0 \int_{\tilde{\Omega}_c} \frac{\partial \boldsymbol{B}_0}{\partial t} \cdot (v\boldsymbol{e}_3) + \int_{\tilde{\Omega}_c} \mathbf{curl}\,\boldsymbol{H}_0 \cdot \mathbf{curl}(v\boldsymbol{e}_3) = 0 \qquad \forall\, v \in C_0^\infty(\tilde{\Omega}_c). \tag{4.10}$$

Moreover, the homogenized $\boldsymbol{H}$-formulation (4.4) shows that

$$\theta_c\sigma_0 \int_{\tilde{\Omega}_c} \frac{\partial \boldsymbol{B}_0}{\partial t} \cdot (v\boldsymbol{e}_1) + \int_{\tilde{\Omega}_c} \mathbf{curl}\,\boldsymbol{H}_0 \cdot \mathbf{curl}(v\boldsymbol{e}_1) = 0 \quad \forall\, v \in C_0^\infty(\tilde{\Omega}_c). \tag{4.11}$$

Then the proof is completed by combining (4.9)–(4.11). ☐

THEOREM 4.7. *Let $\boldsymbol{R}_0$ be the weak limit of $\boldsymbol{R}_\epsilon$ in $\boldsymbol{L}^2(0,T;\boldsymbol{H}(\mathbf{curl},\Omega))$ and $\boldsymbol{H}_0 = \boldsymbol{R}_0 + \boldsymbol{H}_s$. Then the homogenized Maxwell's equations hold in distributional sense*

$$\frac{\partial \boldsymbol{B}_0}{\partial t} + \mathbf{curl}\,\boldsymbol{E}_0 = 0 \quad \text{in } \Omega, \tag{4.12a}$$

$$\mathbf{curl}\,\boldsymbol{H}_0 = \underline{\underline{\sigma}}\boldsymbol{E}_0 + \boldsymbol{J}_s \quad \text{in } \Omega, \tag{4.12b}$$

$$\boldsymbol{H}_0(\cdot,0) = 0 \quad \text{in } \Omega, \tag{4.12c}$$

$$\boldsymbol{E}_0 \times \boldsymbol{n} = 0 \quad \text{on } \Gamma, \tag{4.12d}$$

where $\underline{\underline{\sigma}}$ *is the homogenized anisotropic conductivity defined by*

$$\underline{\underline{\sigma}} \equiv \theta_c \begin{pmatrix} 0 & & \\ & \sigma_0 & \\ & & \sigma_0 \end{pmatrix} \quad \textit{in } \tilde{\Omega}_c, \qquad \underline{\underline{\sigma}} \equiv \begin{pmatrix} 0 & & \\ & 0 & \\ & & 0 \end{pmatrix} \quad \textit{elsewhere.}$$

Proof. First we note the following facts:

- (4.12a) is obvious by (4.6) and (4.7),
- (4.12c) is obvious by Lemma 3.6, and
- (4.12d) is obvious by (4.7) and $\boldsymbol{A}_0 \times \boldsymbol{n} = 0$ on Γ.

Now it is left to prove (4.12b).

For any $\boldsymbol{w} \in \boldsymbol{C}_0^\infty(\tilde{\Omega}_c)$, there exist a $\boldsymbol{\Phi} \in \boldsymbol{H}_0(\mathbf{curl}, \tilde{\Omega}_c)$ and a $\phi \in H_0^1(\tilde{\Omega}_c)$ such that $\boldsymbol{w} = \mathbf{curl}\, \boldsymbol{v} + \nabla\phi$. Notice that $\operatorname{div} \boldsymbol{E}_0 = 0$ because of $\operatorname{div} \boldsymbol{A}_0 = 0$. Then

$$\begin{aligned} \int_{\tilde{\Omega}_c} (\mathbf{curl}\, \boldsymbol{H}_0 - \theta_c\sigma_0\boldsymbol{E}_0) \cdot \boldsymbol{w} &= \int_{\tilde{\Omega}_c} (\mathbf{curl}\, \boldsymbol{H}_0 - \theta_c\sigma_0\boldsymbol{E}_0) \cdot \mathbf{curl}\, \boldsymbol{v} \\ &= \int_{\tilde{\Omega}_c} \left(\mathbf{curl}\, \boldsymbol{H}_0 \cdot \mathbf{curl}\, \boldsymbol{v} + \theta_c\sigma_0\, \mathbf{curl}\, \frac{\partial \boldsymbol{A}_0}{\partial t} \cdot \boldsymbol{v} \right) \\ &= \int_{\tilde{\Omega}_c} \left(\mathbf{curl}\, \boldsymbol{H}_0 \cdot \mathbf{curl}\, \boldsymbol{v} + \theta_c\sigma_0 \frac{\partial \boldsymbol{B}_0}{\partial t} \cdot \boldsymbol{v} \right) = 0. \end{aligned}$$

Since $\boldsymbol{w}$ is arbitrary, we find that

$$\theta_c\sigma_0\boldsymbol{E}_0 = \mathbf{curl}\, \boldsymbol{H}_0 = \mathbf{curl}(u\boldsymbol{e}_1) = \left(0, \frac{\partial u}{\partial x_3}, -\frac{\partial u}{\partial x_2}\right) \qquad \text{in } \tilde{\Omega}_c\ .$$

The above equality can also be written as

$$\mathbf{curl}\, \boldsymbol{H}_0 = \underline{\underline{\sigma}}\boldsymbol{E}_0 \qquad \text{in } \tilde{\Omega}_c\ .$$

On the other hand, it's easy to see that

$$\mathbf{curl}\, \boldsymbol{H}_0 = \mathbf{curl}\, \boldsymbol{H}_s = \boldsymbol{J}_s \quad \text{in } \tilde{\Omega}_{nc}.$$

Adding up the above two identities leads to (4.12b). ◻

4.3. The homogenized $\boldsymbol{A}$-formulation. From (4.7) and (4.12b), we obtain a weak formulation: Find $\boldsymbol{A} \in \boldsymbol{L}^2(0, T; \boldsymbol{H}_0(\mathbf{curl}, \Omega))$ such that $\boldsymbol{A}(\cdot, 0) = 0$ and

$$\int_\Omega \underline{\underline{\sigma}} \frac{\partial \boldsymbol{A}}{\partial t} \cdot \boldsymbol{v} + \int_\Omega \mu_0^{-1}\, \mathbf{curl}\, \boldsymbol{A} \cdot \mathbf{curl}\, \boldsymbol{v} = \int_\Omega \boldsymbol{J}_s \cdot \boldsymbol{v} \quad \forall \boldsymbol{v} \in \boldsymbol{H}_0(\mathbf{curl}, \Omega). \tag{4.13}$$

Clearly the homogenized potential $\boldsymbol{A}_0$ solves (4.13). But similar to the micro-scale problem, the solution of (4.13) is not unique.

Lemma 4.8. *Define*

$$\begin{aligned} \boldsymbol{V}_0 &:= \left\{ \boldsymbol{v} \in \boldsymbol{H}_0(\mathbf{curl}, \Omega) : (\boldsymbol{v}, \nabla p) = 0 \quad \forall\, p \in \tilde{V} \right\}, \\ \tilde{V} &:= \left\{ p \in H_0^1(\Omega) :\ p = p(x_1) \quad \textit{in } \tilde{\Omega}_c \right\}. \end{aligned}$$

Then $\boldsymbol{V}_0$ *is a Hilbert space equipped with the inner product and norm*

$$(\boldsymbol{v}, \boldsymbol{w})_{\boldsymbol{V}_0} = \int_{\tilde{\Omega}_c} (v_2 w_2 + v_3 w_3) + \int_\Omega \mathbf{curl}\, \boldsymbol{v} \cdot \mathbf{curl}\, \boldsymbol{w}, \qquad \|\boldsymbol{v}\|_{\boldsymbol{V}_0} = \sqrt{(\boldsymbol{v}, \boldsymbol{v})_{\boldsymbol{V}_0}}\ ,$$

Proof. We need only prove that $\|\boldsymbol{v}\|_{\boldsymbol{V}_0} = 0$ implies $\boldsymbol{v} = 0$ for any $\boldsymbol{v} \in \boldsymbol{V}_0$. Since Ω is simply-connected, $\mathbf{curl}\,\boldsymbol{v} = 0$ indicates that $\boldsymbol{v} = \operatorname{grad}\phi$ for some $\phi \in H_0^1(\Omega)$. Then

$$\frac{\partial \phi}{\partial x_i} = v_i = 0 \qquad \text{in } \tilde{\Omega}_c, \quad i = 2, 3.$$

This means that $\phi \in \tilde{V}$. We conclude $\boldsymbol{v} = 0$ from the definition of $\boldsymbol{V}_0$. □

A modified weak formulation of (4.12) reads: Find $\boldsymbol{a} \in \boldsymbol{L}^2(0, T; \boldsymbol{V}_0)$ such that $\boldsymbol{a}(\cdot, 0) = 0$ in $\tilde{\Omega}_c$ and

$$\int_\Omega \underline{\underline{\sigma}} \frac{\partial \boldsymbol{a}}{\partial t} \cdot \boldsymbol{v} + \int_\Omega \mu_0^{-1}\, \mathbf{curl}\,\boldsymbol{a} \cdot \mathbf{curl}\,\boldsymbol{v} = \int_\Omega \boldsymbol{J}_s \cdot \boldsymbol{v} \qquad \forall\, \boldsymbol{v} \in \boldsymbol{V}_0. \tag{4.14}$$

THEOREM 4.9. *Let $\boldsymbol{A}_0$ be the vector potential defined in* (4.6). *Then $\boldsymbol{a} = \boldsymbol{A}_0$ is the unique solution of problem* (4.14).

Proof. From (4.6), it is obvious that $\boldsymbol{A}_0 \in \boldsymbol{V}_0$. Since $\boldsymbol{A}_0$ solves (4.13), it also solves (4.14). The proof for the uniqueness is similar to that for parabolic problems and is omitted here. □

THEOREM 4.10. *Let $\boldsymbol{a}_\epsilon$, $\boldsymbol{a}$ be the solutions of* (3.10) *and* (4.14) *respectively. Then*

$$\lim_{\epsilon \to 0} \sigma_\epsilon \frac{\partial \boldsymbol{a}_\epsilon}{\partial t} = \underline{\underline{\sigma}} \frac{\partial \boldsymbol{a}}{\partial t} \qquad \textit{weakly in} \quad \boldsymbol{L}^2(0, T; \boldsymbol{L}^2(\Omega))\ ,$$
$$\lim_{\epsilon \to 0} \mathbf{curl}\,\boldsymbol{a}_\epsilon = \mathbf{curl}\,\boldsymbol{a} \qquad \textit{strongly in} \quad \boldsymbol{L}^2(0, T; \boldsymbol{L}^2(\Omega))\ .$$

Proof. From (3.12), (3.5), and (2.4b), we deduce that

$$\sigma_\epsilon \frac{\partial \boldsymbol{a}_\epsilon}{\partial t} = -\sigma_\epsilon \boldsymbol{E}_\epsilon = \boldsymbol{J}_s - \mathbf{curl}\,\boldsymbol{H}_\epsilon = \mathbf{curl}\,\boldsymbol{R}_\epsilon\ .$$

Then (3.25) and Lemma 3.7 show that

$$\lim_{\epsilon \to 0} \sigma_\epsilon \frac{\partial \boldsymbol{a}_\epsilon}{\partial t} = -\,\mathbf{curl}\,\boldsymbol{u}_0 = -\,\mathbf{curl}\,\boldsymbol{R}_0 \qquad \text{weakly in} \quad \boldsymbol{L}^2(0, T; \boldsymbol{L}^2(\Omega))\ .$$

Since $\mathbf{curl}\,\boldsymbol{R}_0 = \boldsymbol{J}_s - \mathbf{curl}\,\boldsymbol{H}_0$, (4.12b) and (4.7) imply that

$$\lim_{\epsilon \to 0} \sigma_\epsilon \frac{\partial \boldsymbol{a}_\epsilon}{\partial t} = -\underline{\underline{\sigma}} \boldsymbol{E}_0 = \underline{\underline{\sigma}} \frac{\partial \boldsymbol{A}_0}{\partial t} = \underline{\underline{\sigma}} \frac{\partial \boldsymbol{a}}{\partial t} \qquad \text{weakly in} \quad \boldsymbol{L}^2(0, T; \boldsymbol{L}^2(\Omega))\ .$$

Now notice that

$$\mathbf{curl}\,\boldsymbol{a}_\epsilon = \mathbf{curl}\,\boldsymbol{A}_\epsilon = \mu_0(\boldsymbol{R}_\epsilon + \boldsymbol{H}_s),$$
$$\mathbf{curl}\,\boldsymbol{a} = \mathbf{curl}\,\boldsymbol{A}_0 = \mu_0(\boldsymbol{R}_0 + \boldsymbol{H}_s).$$

From Lemma 4.1 we have

$$\lim_{\epsilon \to 0} \|\mathbf{curl}(\boldsymbol{a}_\epsilon - \boldsymbol{a})\|_{\boldsymbol{L}^2(0,T;\boldsymbol{L}^2(\Omega))} = \mu_0 \lim_{\epsilon \to 0} \|\boldsymbol{R}_\epsilon - \boldsymbol{R}_0\|_{\boldsymbol{L}^2(0,T;\boldsymbol{L}^2(\Omega))} = 0.$$

The proof is completed. □

5. Nonlinear eddy current problems. In this section, we shall study the nonlinear eddy current problem where $\boldsymbol{B}_\epsilon(\cdot)$ satisfies (H1). Unfortunately we have not proven the strong convergence of $\boldsymbol{R}_\epsilon$ to $\boldsymbol{R}_0$ for $\epsilon_f > 0$. The strong convergence plays an important role in our homogenization theory. In this section, we make an additional assumption

$$\theta_c = 1, \quad \theta_f = 0. \tag{5.1}$$

The insulating film has zero thickness but still prevents eddy currents from passing through laminations. In this case, Ω_c has inner boundaries, namely,

$$\begin{aligned} &\Omega_c = \bigcup_{i=1}^{M} \Omega_i, \qquad \Omega_i = \big(X_i,\ X_{i+1}\big) \times \big(0,\ L_2\big) \times \big(0,\ L_3\big), \\ &\tilde{\Omega}_c = \big(X_1,\ X_{M+1}\big) \times \big(0,\ L_2\big) \times \big(0,\ L_3\big). \end{aligned}$$

This is reasonable in electrical engineering (see Fig. 1.2). In fact, Li and Zheng proposed an approximate $\boldsymbol{H}$-formulation by omitting coating films [22]. They proved that the approximate solution converges to the exact solution as the film thickness tends to zero. In this section, we only study the homogenized $\boldsymbol{H}$-formulation of the nonlinear eddy current problem.

Since $\epsilon_f = 0$, from (H1) we find that $\boldsymbol{B}_\epsilon(\boldsymbol{H}) = \boldsymbol{f}_{\mathrm{BH}}(\boldsymbol{H})$. The $\boldsymbol{H}$-formulation (3.3) turns out to be: Find $\boldsymbol{R}_\epsilon \in \boldsymbol{L}^2(0,T;\mathbf{U}_\epsilon)$ such that $\boldsymbol{R}_\epsilon(\cdot,0) = 0$ and

$$\sigma_0 \int_\Omega \frac{\partial}{\partial t} \boldsymbol{f}_{\mathrm{BH}}(\boldsymbol{R}_\epsilon + \boldsymbol{H}_s) \cdot \boldsymbol{v} + \int_\Omega \mathbf{curl}\, \boldsymbol{R}_\epsilon \cdot \mathbf{curl}\, \boldsymbol{v} = 0 \qquad \forall\, \boldsymbol{v} \in \mathbf{U}_\epsilon. \tag{5.2}$$

From [22], the theories in Section 3 are still true. We shall adopt the same notation for convenience.

We start from the decomposition of the reaction field $\boldsymbol{R}_\epsilon = \boldsymbol{u}_\epsilon + \nabla\psi_\epsilon$. Since $\boldsymbol{u}_\epsilon \in \boldsymbol{H}_0(\mathbf{curl},\Omega_c) \subset \boldsymbol{H}_0(\mathbf{curl},\tilde{\Omega}_c)$, there exist a $\zeta_\epsilon \in H_0^1(\tilde{\Omega}_c)$ and a $\boldsymbol{w}_\epsilon \in \boldsymbol{H}_0(\mathbf{curl},\tilde{\Omega}_c)$ such that

$$\begin{aligned} &\boldsymbol{u}_\epsilon = \nabla\zeta_\epsilon + \boldsymbol{w}_\epsilon, \qquad \operatorname{div} \boldsymbol{w}_\epsilon = 0 \quad \text{in} \ \tilde{\Omega}_c, \\ &\|\zeta_\epsilon\|_{H^1(\tilde{\Omega}_c)} + \|\boldsymbol{w}_\epsilon\|_{\boldsymbol{H}(\mathbf{curl},\tilde{\Omega}_c)} \le C \|\boldsymbol{u}_\epsilon\|_{\boldsymbol{H}(\mathbf{curl},\Omega)}, \end{aligned}$$

where the constant C depends on $\tilde{\Omega}_c$ but is independent of ϵ. Write $\hat{\psi}_\epsilon = \psi_\epsilon + \zeta_\epsilon$. It follows that

$$\begin{aligned} &\boldsymbol{R}_\epsilon = \nabla\hat{\psi}_\epsilon + \boldsymbol{w}_\epsilon, \qquad \int_\Omega \boldsymbol{w}_\epsilon \cdot \nabla\hat{\psi}_\epsilon = -\int_{\tilde{\Omega}_c} (\operatorname{div} \boldsymbol{w}_\epsilon)\hat{\psi}_\epsilon = 0, \\ &\left\|\hat{\psi}_\epsilon\right\|_{H^1(\Omega)} + \|\boldsymbol{w}_\epsilon\|_{\boldsymbol{H}(\mathbf{curl},\tilde{\Omega}_c)} \le \|\psi_\epsilon\|_{H^1(\Omega)} + \|\boldsymbol{u}_\epsilon\|_{\boldsymbol{H}(\mathbf{curl},\tilde{\Omega}_c)} \le C \|\boldsymbol{R}_\epsilon\|_{\boldsymbol{H}(\mathbf{curl},\Omega)}. \end{aligned}$$

Since $\tilde{\Omega}_c$ is a convex polyhedron, the embedding theorem in [2] indicates that $\boldsymbol{w}_\epsilon \in \boldsymbol{H}^1(\tilde{\Omega}_c)$ and

$$\|\boldsymbol{w}_\epsilon\|_{\boldsymbol{H}^1(\tilde{\Omega}_c)} \le C \|\boldsymbol{w}_\epsilon\|_{\boldsymbol{H}(\mathbf{curl},\tilde{\Omega}_c)} \le C \|\boldsymbol{R}_\epsilon\|_{\boldsymbol{H}(\mathbf{curl},\tilde{\Omega}_c)}.$$

Since $\operatorname{div} \boldsymbol{w}_\epsilon = 0$ and $\boldsymbol{u}_\epsilon \in \boldsymbol{H}^1(0,T;\boldsymbol{L}^2(\tilde{\Omega}_c))$, we also have

$$\|\boldsymbol{w}_\epsilon\|_{\boldsymbol{H}^1\left(0,T;\boldsymbol{L}^2(\tilde{\Omega}_c)\right)} \le C \|\boldsymbol{u}_\epsilon\|_{\boldsymbol{H}^1\left(0,T;\boldsymbol{L}^2(\tilde{\Omega}_c)\right)}, \qquad \operatorname{div} \frac{\partial \boldsymbol{w}_\epsilon}{\partial t} = 0 \quad \text{in} \ \tilde{\Omega}_c\,.$$

Introduce the Sobolev-Bochner space (cf. [24, Section 7.1])

$$\boldsymbol{W}^{1,2,2}\big(0,T;\boldsymbol{H}^1(\Omega),\boldsymbol{L}^2(\Omega)\big)=\Big\{\boldsymbol{v}\in\boldsymbol{L}^2(0,T;\boldsymbol{H}^1(\Omega)):\frac{\partial\boldsymbol{v}}{\partial t}\in\boldsymbol{L}^2(0,T;\boldsymbol{L}^2(\Omega))\Big\},$$

which is equipped with the following norm

$$\|\boldsymbol{v}\|_{\boldsymbol{W}^{1,2,2}\left(0,T;\boldsymbol{H}^1(\Omega),\boldsymbol{L}^2(\Omega)\right)}=\left(\|\boldsymbol{v}\|^2_{\boldsymbol{L}^2(0,T;\boldsymbol{H}^1(\Omega))}+\left\|\frac{\partial\boldsymbol{v}}{\partial t}\right\|^2_{\boldsymbol{L}^2(0,T;\boldsymbol{L}^2(\Omega))}\right)^{1/2}.$$

Next we shall examine the strong convergence of $\{\boldsymbol{R}_\epsilon\}_{\epsilon>0}$. For convenience, the same notation will also denote their subsequences without causing confusion.

Lemma 5.1. *Let $\boldsymbol{R}_\epsilon$ be the solution of problem* (3.3) *and let $\boldsymbol{R}_0$ be the weak limit of $\boldsymbol{R}_\epsilon$ in* (3.14). *Then*

$$\lim_{\epsilon\to0}\|\boldsymbol{R}_\epsilon-\boldsymbol{R}_0\|_{\boldsymbol{L}^2(0,T;\boldsymbol{L}^2(\Omega))}=0. \tag{5.3}$$

Proof. First we prove the strong convergence of the regular functions $\{\boldsymbol{w}_\epsilon\}_{\epsilon>0}$. An application of (3.17) yields

$$\|\boldsymbol{w}_\epsilon\|_{\boldsymbol{L}^2\left(0,T;\boldsymbol{H}^1(\tilde\Omega_c)\right)}\le C\,\|\boldsymbol{u}_\epsilon\|_{\boldsymbol{L}^2\left(0,T;\boldsymbol{H}(\mathbf{curl},\tilde\Omega_c)\right)}\le C\ .$$

Thus there exists a constant C independent of ϵ such that

$$\|\boldsymbol{w}_\epsilon\|_{\boldsymbol{W}^{1,2,2}\left(0,T;\boldsymbol{H}^1(\tilde\Omega_c),\boldsymbol{L}^2(\tilde\Omega_c)\right)}\le\|\boldsymbol{w}_\epsilon\|_{\boldsymbol{L}^2\left(0,T;\boldsymbol{H}^1(\tilde\Omega_c)\right)}+\|\boldsymbol{w}_\epsilon\|_{\boldsymbol{H}^1\left(0,T;\boldsymbol{L}^2(\tilde\Omega_c)\right)}\le C.$$

By the compact embedding (cf. [24, Lemma 7.7])

$$\boldsymbol{W}^{1,2,2}\big(0,T;\boldsymbol{H}^1(\tilde\Omega_c),\boldsymbol{L}^2(\tilde\Omega_c)\big)\Subset\boldsymbol{L}^2\big(0,T;\boldsymbol{L}^2(\tilde\Omega_c)\big),$$

there exists a subsequence of $\{\boldsymbol{w}_\epsilon\}_{\epsilon>0}$ and a limit $\boldsymbol{w}_0$ such that

$$\lim_{\epsilon\to0}\boldsymbol{w}_\epsilon=\boldsymbol{w}_0\qquad\begin{array}{l}\text{strongly in }\boldsymbol{L}^2\big(0,T;\boldsymbol{L}^2(\tilde\Omega_c)\big),\\ \text{weakly in }\boldsymbol{W}^{1,2,2}\big(0,T;\boldsymbol{H}^1(\tilde\Omega_c),\boldsymbol{L}^2(\tilde\Omega_c)\big).\end{array} \tag{5.4}$$

To prove the strong convergence of $\boldsymbol{R}_\epsilon$, we shall utilize the divergence-free property of the magnetic flux density. Taking $\boldsymbol{v}=\nabla\varphi$ in (3.3) shows that

$$\int_\Omega\frac{\partial}{\partial t}\boldsymbol{f}_{\rm BH}(\boldsymbol{H}_\epsilon)\cdot\nabla\varphi=0\qquad\forall\,\varphi\in H^1(\Omega)\ .$$

Combining with the initial condition in (2.4), we find that

$$\operatorname{div}\boldsymbol{f}_{\rm BH}(\boldsymbol{H}_\epsilon)=0\quad\text{in }\ \Omega\times(0,\ T),\qquad\boldsymbol{f}_{\rm BH}(\boldsymbol{H}_\epsilon)\cdot\boldsymbol{n}=0\quad\text{on }\ \Gamma\times(0,\ T). \tag{5.5}$$

By (2.3) and the weak convergence of $\boldsymbol{R}_\epsilon$, we deduce that

$$\begin{aligned}&\mu_{\min}\lim_{\epsilon\to0}\|\boldsymbol{R}_\epsilon-\boldsymbol{R}_0\|^2_{\boldsymbol{L}^2(0,T;\boldsymbol{L}^2(\Omega))}\\ &\quad\le\lim_{\epsilon\to0}\int_0^T\int_\Omega[\boldsymbol{f}_{\rm BH}(\boldsymbol{H}_\epsilon)-\boldsymbol{f}_{\rm BH}(\boldsymbol{H}_0)]\cdot(\boldsymbol{H}_\epsilon-\boldsymbol{H}_0)\\ &\quad=\lim_{\epsilon\to0}\int_0^T\int_\Omega\boldsymbol{f}_{\rm BH}(\boldsymbol{H}_\epsilon)\cdot(\boldsymbol{H}_\epsilon-\boldsymbol{H}_0)=\lim_{\epsilon\to0}\int_0^T\int_\Omega\boldsymbol{f}_{\rm BH}(\boldsymbol{H}_\epsilon)\cdot(\boldsymbol{w}_\epsilon-\boldsymbol{w}_0)=0.\end{aligned}$$

This completes the proof. ∎

THEOREM 5.2. *Let $\boldsymbol{R}_0 = \nabla\psi_0 + u\boldsymbol{e}_1$ be the limit of $\boldsymbol{R}_\epsilon$. It solves the homogenized problem: Find $\boldsymbol{R}_0 \in \boldsymbol{L}^2(0,T;\boldsymbol{X}_0)$ such that $\boldsymbol{R}_0(\cdot,0) = 0$ and*

$$\sigma_0 \int_\Omega \frac{\partial}{\partial t}\boldsymbol{f}_{\rm BH}(\boldsymbol{R}_0 + \boldsymbol{H}_s)\cdot\boldsymbol{v} + \int_\Omega \mathbf{curl}\,\boldsymbol{R}_0\cdot\mathbf{curl}\,\boldsymbol{v} = 0 \qquad \forall\,\boldsymbol{v}\in\boldsymbol{X}_0. \tag{5.6}$$

Proof. Take any $\boldsymbol{v}\in\boldsymbol{C}_0^\infty(0,T;\boldsymbol{X}_0)$. Clearly (5.2) shows that

$$\sigma_0 \int_0^T\int_\Omega \frac{\partial}{\partial t}\boldsymbol{f}_{\rm BH}(\boldsymbol{R}_\epsilon + \boldsymbol{H}_s)\cdot\boldsymbol{v} + \int_0^T\int_\Omega \mathbf{curl}\,\boldsymbol{R}_\epsilon\cdot\mathbf{curl}\,\boldsymbol{v} = 0\,.$$

From (3.18)–(3.20), we know that

$$\lim_{\epsilon\to 0}\int_0^T\int_\Omega \mathbf{curl}\,\boldsymbol{R}_\epsilon\cdot\mathbf{curl}\,\boldsymbol{v} = \int_0^T\int_\Omega \mathbf{curl}\,\boldsymbol{R}_0\cdot\mathbf{curl}\,\boldsymbol{v}.$$

From Lemma 5.1 and the formula of integral by part in t, we have

$$\lim_{\epsilon\to 0}\int_0^T\int_\Omega \frac{\partial}{\partial t}\boldsymbol{B}(\boldsymbol{R}_\epsilon + \boldsymbol{H}_s)\cdot\boldsymbol{v} = \int_0^T\int_\Omega \frac{\partial}{\partial t}\boldsymbol{B}(\boldsymbol{R}_0 + \boldsymbol{H}_s)\cdot\boldsymbol{v}.$$

Taking the limit of (5.2) and using the two equalities above, we obtain

$$\sigma_0 \int_0^T\int_\Omega \frac{\partial}{\partial t}\boldsymbol{B}(\boldsymbol{R}_0 + \boldsymbol{H}_s)\cdot\boldsymbol{v} + \int_0^T\int_\Omega \mathbf{curl}\,\boldsymbol{R}_0\cdot\mathbf{curl}\,\boldsymbol{v} = 0 \quad \forall\,\boldsymbol{v}\in\boldsymbol{C}_0^\infty(0,T;\boldsymbol{X}_0).$$

Then the density of $\boldsymbol{C}_0^\infty(0,T;\boldsymbol{X}_0)$ in $\boldsymbol{L}^2(0,T;\boldsymbol{X}_0)$ indicates that $\boldsymbol{R}_0$ solves (5.6) in a distributional sense. The initial condition has been verified in Lemma 3.6. ∎

6. Homogenized $\boldsymbol{H}$-formulation for multiply-connected conductors.

It is well-known that the $\boldsymbol{H}$-formulation becomes complicated when dealing with multiply-connected conductors (see e.g. Fig. 6.1 right), since the scalar potential is discontinuous in nonconducting region. In this section, we shall propose a homogenized $\boldsymbol{H}$-formulation for multiply-connected conductors.

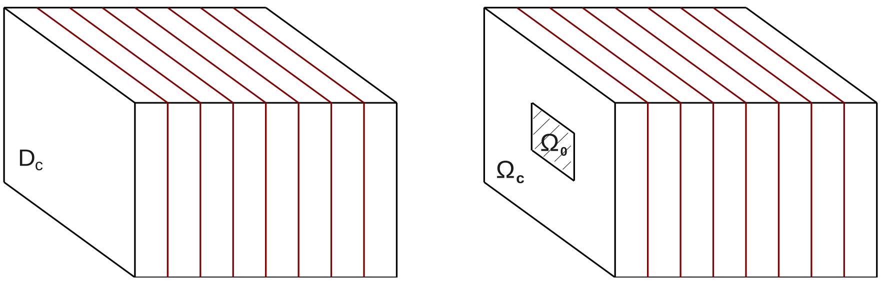

FIG. 6.1. *Left: simply-connected virtual laminations. Right: multiply-connected physical laminations.*

First we introduce two types of laminations, *virtual laminations and physical laminations*, as follows:

1. Virtual laminations: the laminations are simply connected and defined as follows (see Fig. 6.1 left)

$$
\begin{aligned}
&D_c = \bigcup_{i=1}^{M} D_i, \qquad D_i = \big(X_i + \epsilon_f,\ X_{i+1} - \epsilon_f\big) \times \big(0,\ L_2\big) \times \big(0,\ L_3\big),\\
&\tilde{D}_c = \big(0, L_1\big) \times \big(0,\ L_2\big) \times \big(0,\ L_3\big).
\end{aligned}
$$

2. Physical laminations: the laminations are multiply connected and defined by (see Fig. 6.1 right)

$$
\begin{aligned}
&\Omega_c = \bigcup_{i=1}^{M} \Omega_i, \qquad \tilde{\Omega}_c = \tilde{D}_c \backslash \bar{\Omega}_0,\\
&\Omega_0 = (0, L_1) \times (Y_1, Y_2) \times (Z_1, Z_2)\,, \qquad \Omega_i = D_i \backslash \bar{\Omega}_0, \quad 1 \le i \le M,
\end{aligned}
$$

   where $0 < Y_1 < Y_2 < L_2$ and $0 < Z_1 < Z_2 < L_3$.

We remark that the theories in this section can be extended directly to laminations with multiple holes, namely,

$$
\begin{aligned}
&\Omega_0 = \bigcup_{i=1}^{I} \bigcup_{j=1}^{J} (0, L_1) \times (Y_{2i-1}, Y_{2i}) \times (Z_{2j-1}, Z_{2j})\,,\\
&0 < Y_1 < \cdots < Y_{2I} < L_2, \quad 0 < Z_1 < \cdots < Z_{2J} < L_3.
\end{aligned}
$$

First we propose the homogenized $\boldsymbol{H}$-formulation for virtual laminations. Define

$$
\boldsymbol{X}_D := \mathcal{H}_0^1(\tilde{D}_c)\, \boldsymbol{e}_1 + \nabla H^1(\Omega).
$$

Since each D_i is simply-connected, by the theories in Section 4 and 5, the homogenized $\boldsymbol{H}$-formulation reads: Find $\boldsymbol{R}_0 \in \boldsymbol{L}^2(0, T; \boldsymbol{X}_D)$ such that $\boldsymbol{R}_0(\cdot, 0) = 0$ and

$$
\theta_c \sigma_0 \int_\Omega \frac{\partial}{\partial t} \boldsymbol{B}(\boldsymbol{R}_0 + \boldsymbol{H}_s) \cdot \boldsymbol{v} + \int_\Omega \mathbf{curl}\, \boldsymbol{R}_0 \cdot \mathbf{curl}\, \boldsymbol{v} = 0 \qquad \forall\, \boldsymbol{v} \in \boldsymbol{X}_D, \tag{6.1}
$$

where $\theta_c < 1$, $\boldsymbol{B}(\boldsymbol{H}) = \mu_0 \boldsymbol{H}$ for linear problems, and $\theta_c = 1$, $\boldsymbol{B}(\boldsymbol{H}) = \boldsymbol{f}_{\rm BH}(\boldsymbol{H})$ for nonlinear problems.

For physical laminations, notice that $\Omega_0 \subset \Omega \backslash \bar{\Omega}_c$ is a subset of the nonconducting domain. Write $\boldsymbol{R}_0 = \nabla \psi_0 + u \boldsymbol{e}_1$ with $\psi_0 \in H^1(\Omega)$ and $u \in \mathcal{H}_0^1(\tilde{D}_c)$. Then we deduce that

$$
\mathbf{curl}(u \boldsymbol{e}_1) = \mathbf{curl}\, \boldsymbol{R}_0 = 0 \qquad \text{in } \ \Omega_0.
$$

This yields $\dfrac{\partial u}{\partial x_2} = \dfrac{\partial u}{\partial x_3} = 0$, and thus

$$
u = u(x_1) \qquad \text{in } \ \Omega_0. \tag{6.2}
$$

Now we define

$$
\boldsymbol{X}_0 := \Big\{ \nabla \varphi + v \boldsymbol{e}_1 :\ \varphi \in H^1(\Omega),\ \ v \in \mathcal{H}_0^1(\tilde{D}_c) \ \text{ satisfying } \ v = v(x_1) \ \text{ in } \ \Omega_0 \Big\}.
$$

Clearly $\boldsymbol{R}_0 \in \boldsymbol{X}_0$. And it is easy to verify that

$$
\mathbf{curl}\, \boldsymbol{v} = 0 \quad \text{in } \ \Omega_0, \qquad \forall\, \boldsymbol{v} \in \boldsymbol{X}_0.
$$

Then the homogenized $\boldsymbol{H}$-formulation for multiply-connected conductors reads: Find $\boldsymbol{R}_0 \in \boldsymbol{L}^2(0,T;\boldsymbol{X}_0)$ such that $\boldsymbol{R}_0(\cdot,0) = 0$ and

$$\theta_c\sigma_0 \int_\Omega \frac{\partial}{\partial t}\boldsymbol{B}(\boldsymbol{R}_0 + \boldsymbol{H}_s)\cdot\boldsymbol{v} + \int_\Omega \mathbf{curl}\,\boldsymbol{R}_0\cdot\mathbf{curl}\,\boldsymbol{v} = 0 \qquad \forall\,\boldsymbol{v}\in\boldsymbol{X}_0. \tag{6.3}$$

Problem (6.3) can also be written in the form of (4.5).

7. Numerical validation. In this section, we shall validate the homogenized eddy current problem by finite element computation of an engineering benchmark problem—TEAM Workshop Problem 21^c-M1 [10]. Here we only study the finite element approximation of the $\boldsymbol{H}$-formulation: Find $\boldsymbol{R}_0 \in \boldsymbol{L}^2(0,T;\boldsymbol{X}_0)$ such that $\boldsymbol{R}_0(\cdot,0) = 0$ and

$$\theta_c\sigma_0 \int_\Omega \frac{\partial}{\partial t}\boldsymbol{B}(\boldsymbol{R}_0 + \boldsymbol{H}_s)\cdot\boldsymbol{v} + \int_\Omega \mathbf{curl}\,\boldsymbol{R}_0\cdot\mathbf{curl}\,\boldsymbol{v} = 0 \qquad \forall\,\boldsymbol{v}\in\boldsymbol{X}_0, \tag{7.1}$$

where $\theta_c < 1$, $\boldsymbol{B}(\boldsymbol{H}) = \mu_0\boldsymbol{H}$ for linear problems, and $\theta_c = 1$, $\boldsymbol{B}(\boldsymbol{H}) = \boldsymbol{f}_{\mathrm{BH}}(\boldsymbol{H})$ for nonlinear problems.

7.1. Finite element approximation. Let $\mathcal{T}_h$ be a tetrahedral triangulation of Ω such that $\mathcal{T}_h|_{\tilde{D}_c}$, $\mathcal{T}_h|_{\tilde{\Omega}_c}$ also construct the triangulations of $\tilde{D}_c$ and $\tilde{\Omega}_c$ respectively. For any integer $m \ge 0$, let P_m be the space of polynomials of degree at most m, and let Q_m be the space of polynomials of degree at most m in each variable. We define the Lagrange finite element space on $\mathcal{T}_h$ by

$$V(m,\mathcal{T}_h) = \big\{v\in H^1(\Omega):\ v|_K\in P_m(K),\ \forall\,K\in\mathcal{T}_h\big\}.$$

Let $\mathcal{M}_h$ be a hexahedral partition of $\tilde{D}_c$ such that $\mathcal{M}_h|_{\tilde{\Omega}_c}$ also constructs a partition of $\tilde{\Omega}_c$. Define the finite element space on $\mathcal{M}_h$ by

$$\begin{aligned} U(m,\mathcal{M}_h) = \Big\{&v\in\mathcal{H}_0^1(\tilde{D}_c):\ v|_K = v_1(x_1)v_2(x_2,x_3),\\ &v_1\in P_m\left([X_0,X_1]\right),\ v_2\in Q_m\left([Y_0,Y_1]\times[Z_0,Z_1]\right),\\ &\forall\,K=[X_0,X_1]\times[Y_0,Y_1]\times[Z_0,Z_1]\in\mathcal{M}_h\Big\}.\end{aligned}$$

For simply-connected laminations, we have $\tilde{D}_c = \tilde{\Omega}_c$. Then a conforming finite element space is defined by

$$\boldsymbol{U}_h := \nabla V(m+1,\mathcal{T}_h) + U(m,\mathcal{M}_h)\boldsymbol{e}_1.$$

Based on $\boldsymbol{U}_h$, the semi-discrete approximation of (7.1) reads: Find $\boldsymbol{R}_h \in L^2(0,T;\boldsymbol{U}_h)$ such that $\boldsymbol{R}_h(\cdot,0) = 0$ and

$$\theta_c\sigma_0 \int_\Omega \frac{\partial}{\partial t}\boldsymbol{B}(\boldsymbol{R}_h + \boldsymbol{H}_s)\cdot\boldsymbol{v}_h + \int_{\tilde{\Omega}_c} \mathbf{curl}\,\boldsymbol{R}_h\cdot\mathbf{curl}\,\boldsymbol{v}_h = 0 \qquad \forall\,\boldsymbol{v}_h\in\boldsymbol{U}_h. \tag{7.2}$$

The above semi-discrete scheme involves two grids $\mathcal{T}_h$, $\mathcal{M}_h$ and is inconvenient in practical computations. Therefore we come up with another choice — computing u by the Lagrange finite element method on $\mathcal{T}_h$. Define

$$\boldsymbol{V}_h := \nabla V(m+1,\mathcal{T}_h) + \left[V\left(m,\mathcal{T}_h|_{\tilde{\Omega}_c}\right)\cap\mathcal{H}_0^1(\tilde{\Omega}_c)\right]\boldsymbol{e}_1. \tag{7.3}$$

The associated semi-discrete approximation reads: Find $\boldsymbol{R}_h \in L^2(0,T;\boldsymbol{V}_h)$ such that $\boldsymbol{R}_h(\cdot,0) = 0$ and

$$\theta_c\sigma_0 \int_\Omega \frac{\partial}{\partial t}\boldsymbol{B}(\boldsymbol{R}_h + \boldsymbol{H}_s)\cdot\boldsymbol{v}_h + \int_{\tilde{\Omega}_c} \mathbf{curl}\,\boldsymbol{R}_h\cdot\mathbf{curl}\,\boldsymbol{v}_h = 0 \qquad \forall\,\boldsymbol{v}_h \in \boldsymbol{V}_h\ . \tag{7.4}$$

Although $\boldsymbol{V}_h$ seems too small to be a good approximation to $\boldsymbol{X}_0$, (7.4) yields accurate results in numerical experiments (see Section 7.3).

For multiply-connected conductors, we define

$$\begin{aligned}\hat{U}_h &= \{v \in U(m,\mathcal{M}_h):\ v = v(x_1)\ \text{ in }\ \Omega_0\},\\ \hat{V}_h &= \left\{v \in V\left(m, \mathcal{T}_h|_{\tilde{D}_c}\right):\ v = v(x_1)\ \text{ in }\ \Omega_0\right\} \cap \mathcal{H}_0^1(\tilde{D}_c).\end{aligned}$$

The associated conforming finite element spaces are defined by

$$\hat{\boldsymbol{U}}_h = \nabla V(m+1,\mathcal{T}_h) + \hat{U}_h\boldsymbol{e}_1, \qquad \hat{\boldsymbol{V}}_h = \nabla V(m+1,\mathcal{T}_h) + \hat{V}_h\boldsymbol{e}_1.$$

The finite element approximations for multiply-connected conductors are given by replacing $\boldsymbol{U}_h$, $\boldsymbol{V}_h$ with $\hat{\boldsymbol{U}}_h$, $\hat{\boldsymbol{V}}_h$ respectively in (7.2) and (7.4).

7.2. Damped Newton method. Since we prefer to solve the problem on a single mesh, the rest of the paper will be focused on the discrete problem (7.4). In this section, we present a damped Newton method and an alternating iteration method for solving (7.4).

Let $0 = t_0 < t_1 < \cdots < t_N = T$ be a uniform partition of the time interval $[0,T]$ and denote by $\tau = T/N$ the time step. The fully discrete problem reads: Given $\boldsymbol{R}_0 = 0$, find $\boldsymbol{R}_n \in \boldsymbol{V}_h$, $n > 0$, such that

$$\theta_c\sigma_0 \int_\Omega \frac{\boldsymbol{B}_n - \boldsymbol{B}_{n-1}}{\tau}\cdot\boldsymbol{v}_h + \int_{\tilde{\Omega}_c} \mathbf{curl}\,\boldsymbol{R}_n\cdot\mathbf{curl}\,\boldsymbol{v}_h = 0 \qquad \forall\,\boldsymbol{v}_h \in \boldsymbol{V}_h\ , \tag{7.5}$$

where $\boldsymbol{B}_n = \boldsymbol{B}(\boldsymbol{R}_n + \boldsymbol{H}_s(\cdot,t_n))$.

Let $\boldsymbol{R}_{n,k}$, $k \geq 0$ be the approximate solution of (7.5) at the k^{th} step of damped Newton method. Let $\boldsymbol{H}_{n,k} := \boldsymbol{R}_{n,k} + \boldsymbol{H}_s(t_n)$ and $\boldsymbol{B}_{n,k} = \boldsymbol{B}(\boldsymbol{H}_{n,k})$ be the approximate magnetic field and magnetic flux density respectively. We define the residual functional $\mathcal{F}(\boldsymbol{R}_{n,k})$: $\boldsymbol{V}_h \to \mathbb{R}$ by

$$\langle\mathcal{F}(\boldsymbol{R}_{n,k}),\boldsymbol{v}\rangle := \frac{\theta_c\sigma_0}{\tau}\left(\boldsymbol{B}_{n-1} - \boldsymbol{B}_{n,k},\boldsymbol{v}\right) - (\mathbf{curl}\,\boldsymbol{R}_{n,k},\mathbf{curl}\,\boldsymbol{v}) \quad \forall\,\boldsymbol{v} \in \boldsymbol{V}_h.$$

The differential magnetic permeability at $\boldsymbol{H}_{n,k}$ is defined by

$$\boldsymbol{\mu}_{n,k} := \frac{D\boldsymbol{B}}{D\boldsymbol{H}}\left(\boldsymbol{H}_{n,k}\right) \qquad \text{with} \qquad \frac{D\boldsymbol{B}}{D\boldsymbol{H}} = \left(\frac{\partial B_i}{\partial H_j}\right)_{\substack{1\leq i\leq 3\\ 1\leq j\leq 3}}.$$

Then the linearized error equation reads: Find $\boldsymbol{e}_{n,k} \in \boldsymbol{V}_h$ such that

$$a_{n,k}(\boldsymbol{e}_{n,k},\boldsymbol{v}_h) = \langle\mathcal{F}(\boldsymbol{R}_{n,k}),\boldsymbol{v}_h\rangle \qquad \forall\,\boldsymbol{v}_h \in \boldsymbol{V}_h, \tag{7.6}$$

where the bilinear form $a_{n,k}$: $\boldsymbol{V}_h \times \boldsymbol{V}_h \to \mathbb{R}$ is defined by

$$a_{n,k}(\boldsymbol{v},\boldsymbol{w}) := \frac{\theta_c\sigma_0}{\tau}(\boldsymbol{\mu}_{n,k}\boldsymbol{v},\boldsymbol{w}) + (\mathbf{curl}\,\boldsymbol{v},\mathbf{curl}\,\boldsymbol{w}).$$

Given $0 < \rho_{n,k} \leq 1$, the damped Newton method for solving (7.5) reads:

$$\boldsymbol{R}_{n,k+1} = \boldsymbol{R}_{n,k} + \rho_{n,k}\boldsymbol{e}_{n,k}, \qquad k = 0, 1, 2, \cdots . \tag{7.7}$$

Now we present a simple algorithm of damped Newton method.

ALGORITHM 7.1 (Damped Newton Method).
Given the tolerance $0 < \texttt{TOL} \ll 1$ and a factor $\delta = 0.618$.

1. Set $\boldsymbol{R}_{n,0} := \boldsymbol{R}_{n-1}$ and $k = 0$.
2. While $\left\|\mathcal{F}(\boldsymbol{R}_{n,k})\right\|_{\boldsymbol{V}_h'} \geq \texttt{TOL}$ do
   (a) solve the linearized problem (7.6) for an approximate solution $\hat{\boldsymbol{e}}_{n,k}$;
   (b) set $\rho = \delta^{-1}$ and $\hat{\boldsymbol{R}}_{n,k} = \boldsymbol{R}_{n,k}$;
   (c) while $\left\|\mathcal{F}(\hat{\boldsymbol{R}}_{n,k})\right\|_{\boldsymbol{V}_h'} \geq \left\|\mathcal{F}(\boldsymbol{R}_{n,k})\right\|_{\boldsymbol{V}_h'}$ do
      - reduce the step size: $\rho \leftarrow \delta\rho$,
      - correct the approximate solution: $\hat{\boldsymbol{R}}_{n,k} \leftarrow \boldsymbol{R}_{n,k} + \rho\,\hat{\boldsymbol{e}}_{n,k}$,

      end while
   (d) set $\boldsymbol{R}_{n,k+1} \leftarrow \hat{\boldsymbol{R}}_{n,k}$ and $k \leftarrow k+1$.

   end While
3. Set $\boldsymbol{R}_n \leftarrow \boldsymbol{R}_{n,k}$.

Now we study the solution of problem (7.6). For convenience, we write

$$V := V(m+1, \mathcal{T}_h), \qquad V_c := V\left(m, \mathcal{T}_h|_{\tilde{\Omega}_c}\right) \cap \mathcal{H}_0^1(\tilde{\Omega}_c).$$

Since $\boldsymbol{V}_h = \nabla V + V_c\,\boldsymbol{e}_1$, problem (7.6) can be reformulated as: Find $\phi \in V$ and $\theta \in V_c$ such that

$$a_{n,k}(\nabla\phi, \nabla v) + b_{\boldsymbol{\mu}_{n,k}}(v, \theta) = \langle \mathcal{F}(\boldsymbol{R}_{n,k}), \nabla v\rangle \qquad \forall\, v \in V, \tag{7.8}$$

$$a_c(\theta, w) + b_{\boldsymbol{\mu}_{n,k}^T}(\phi, w) = \langle \mathcal{F}(\boldsymbol{R}_{n,k}), w\boldsymbol{e}_1\rangle \qquad \forall\, w \in V_c, \tag{7.9}$$

where

$$b_{\boldsymbol{\mu}}(v, w) := \frac{\theta_c\sigma_0}{\tau}\int_{\Omega_c} (\boldsymbol{\mu}\nabla v)_1\, w,$$

$$a_c(\theta, w) := \int_{\Omega_c}\left(\theta w + \frac{\partial\theta}{\partial x_2}\cdot\frac{\partial w}{\partial x_2} + \frac{\partial\theta}{\partial x_3}\cdot\frac{\partial w}{\partial x_3}\right).$$

Notice that in Step 2 (b) of Algorithm 7.1, we are only solving for an approximate solution of (7.6) or (7.8)–(7.9). This reduces the total computational time greatly and makes the damped Newton method much more efficient compared with that solving (7.6) accurately.

Given an approximate solution $\hat{\boldsymbol{e}}$ of (7.6), we define the residual functional $\mathcal{R}(\hat{\boldsymbol{e}})$: $\boldsymbol{V}_h \to \mathbb{R}$ by

$$\langle \mathcal{R}(\hat{\boldsymbol{e}}), \boldsymbol{v}\rangle := \langle \mathcal{F}(\boldsymbol{R}_{n,k}), \boldsymbol{v}_h\rangle - a_{n,k}(\hat{\boldsymbol{e}}, \boldsymbol{v}) \qquad \forall\, \boldsymbol{v} \in \boldsymbol{V}_h.$$

Then Step 2 (b) of Algorithm 7.1 is realized via the following alternating iteration algorithm for solving (7.8)–(7.9).

ALGORITHM 7.2 (Alternating Iteration Algorithm).
Given the tolerance $0 < \texttt{TOL} \ll 1$ and the maximal number of iterations $N = 10$.

1. Set the initial guess $\boldsymbol{e}_0 = 0$, $\theta_0 = 0$, and set $l = 0$.
2. While $\|\mathcal{R}(\boldsymbol{e}_l)\|_{\boldsymbol{V}_h'} \geq \texttt{TOL}$ and $l \leq N$ do
   (a) solve the following elliptic problem by 5 iterations of conjugate gradient (CG) method preconditioned by algebraic multigrid (AMG) method: Find $\phi_{l+1} \in V$ such that

$$a_{n,k}(\nabla\phi_{l+1}, \nabla v) = \langle \mathcal{F}(\boldsymbol{R}_{n,k}), \nabla v\rangle - b_{\boldsymbol{\mu}_{n,k}}(v, \theta_l) \qquad \forall\, v \in V;$$

   (b) solve the following elliptic problem by 5 iterations of CG method preconditioned by AMG method: Find $\theta_{l+1} \in V_c$ such that

$$a_c(\theta_{l+1}, w) = \langle F(\boldsymbol{R}_{n,k}), w\boldsymbol{e}_1\rangle - b_{\boldsymbol{\mu}^T_{n,k}}(\phi_{l+1}, w) \qquad \forall\, w \in V_c;$$

   (c) set $\boldsymbol{e}_{l+1} \leftarrow \nabla\phi_{l+1} + \theta_{l+1}\boldsymbol{e}_1$ and $l \leftarrow l + 1$.

   end While
3. Set $\hat{\boldsymbol{e}}_{n,k} = \boldsymbol{e}_l$.

Algorithms 7.2 indicates that the error equation (7.6) only involves the solution of two elliptic problems. In practice, the elliptic problems can be solved efficiently by the Boomer-AMG method (cf. [16]).

7.3. Numerical experiments. Our implementation is based on the adaptive finite element package PHG [26] and the computations are carried out on the cluster LSEC-III of Chinese Academy of Sciences. The numerical experiment is performed for the TEAM Workshop Problem 21^c–M1 (see Fig. 7.1). All experimental data are measured by the R & D Center of Baoding Tianwei Group Co., LTD, China [10].

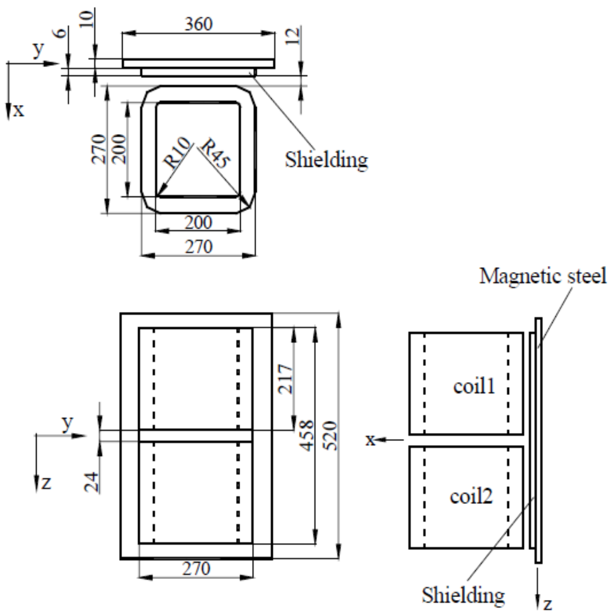

FIG. 7.1. *Geometric sizes of the silicon steel laminations.*

The source currents are carried in opposite directions by two coils and are 3000 Ampere/Turn at a frequency of 50Hz. The conducting region consists of a lamination stack and a magnetic plate whose dimensions are $6 \times 270 \times 458\text{mm}^3$ and $10 \times 360 \times 520\text{mm}^3$ respectively, as shown in Fig. 7.1. The lamination stack consists of 20 simply-connected steel sheets and placed in between the coils and the magnetic plate. The thickness of each steel sheet is 0.3mm. The thickness of the coating film over each sheet is 4μm. We refer to [10] for more details of the model.

Suppose that the steel sheets are laminated together along the x_1-direction. Fig. 7.2 and 7.3 illustrate a cross-section of the lamination stack in the x-z plane. The dash lines represent 20 steel sheets and the solid lines represent finite element partitions. The tetrahedral mesh of the lamination stack is constructed in two steps:

- $\tilde{\Omega}_c$ is subdivided into N layers of cuboid elements ($N = 3$ in Fig. 7.2 and $N = 4$ in Fig. 7.3);
- each cuboid element is subdivided into six tetrahedra.

We set $m = 1$ in (7.3). This means that the first-order and second-order Lagrange finite element spaces are adopted for u and ψ_0 respectively.

The right figures of Fig. 7.2 and 7.3 show the numerical values and experimental values of the first component of the magnetic flux density. The curve with smaller slope represents the values of B_1 at 24 points on the line

$$\{(x, y, z) : \ x = -5.76\,\text{mm}, \ y = 0\,\text{mm}\},$$

and the other curve represents the values of B_1 at 24 points on

$$\{(x, y, z) : \ x = 11.76\,\text{mm}, \ y = 0\,\text{mm}\}.$$

For both figures, the number of partition layers is much less than the number of steel laminations, namely, $N \ll 20$. So the homogenized eddy current model saves computations significantly. And Fig. 7.2–7.3 also show that refining the mesh near the coils improves the computational accuracy considerably.

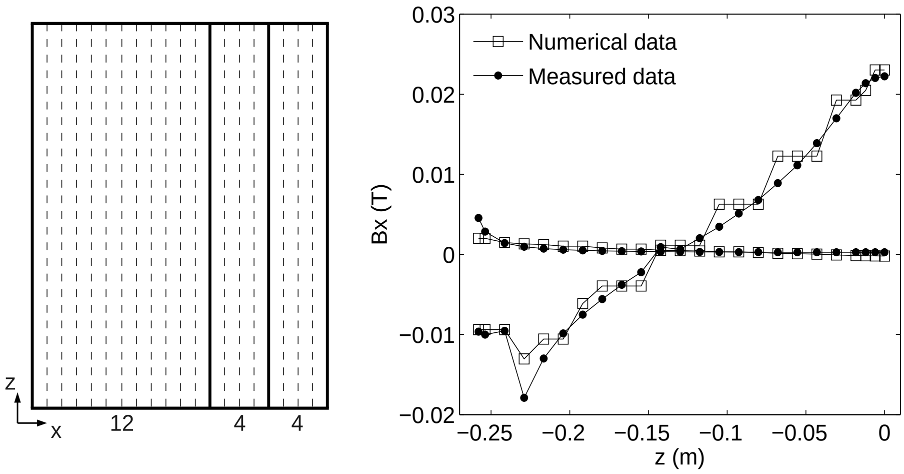

FIG. 7.2. *Left: the lamination stack is divided into $N = 3$ layers of elements in the x_1-direction. Right: numerical and experimental values of B_1 .*

Fig. 7.4 shows the distribution of eddy current density on the cross-section of the lamination stack at $x_1 = 0.0057$ (inside the second lamination from the source side). Fig. 7.5 shows the distribution of eddy current density on two cross-sections of the

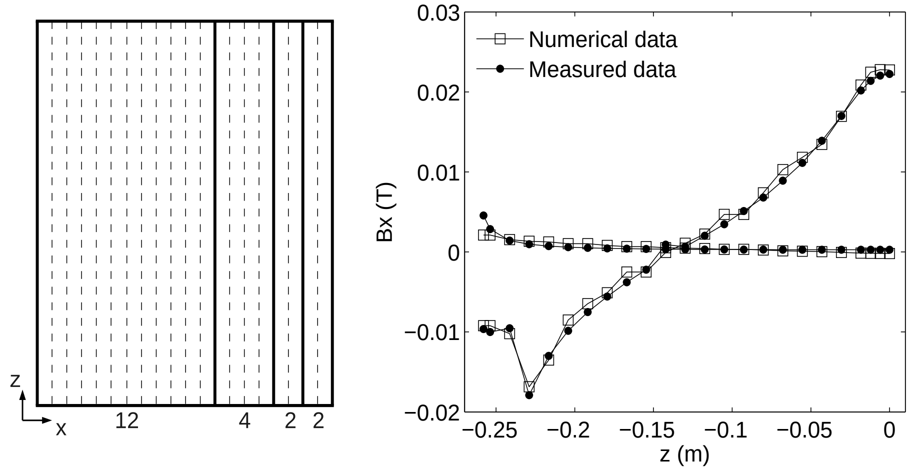

FIG. 7.3. *Left: the lamination stack is divided into $N = 4$ layers of elements in the x_1-direction. Right: numerical and experimental values of B_1 .*

magnetic plate which are at $x_1 = -0.001$ and $x_1 = -0.009$ respectively. Since the cross-section at $x_1 = -0.001$ is close to the lamination stack, Fig. 7.5 (Left) shows a clearly shielded area by the laminations. But the magnetic flux still penetrates into the plate from the opposite side, and yields stronger eddy current density on the cross-section at $x = -0.009$ (Fig. 7.5 (Right)).

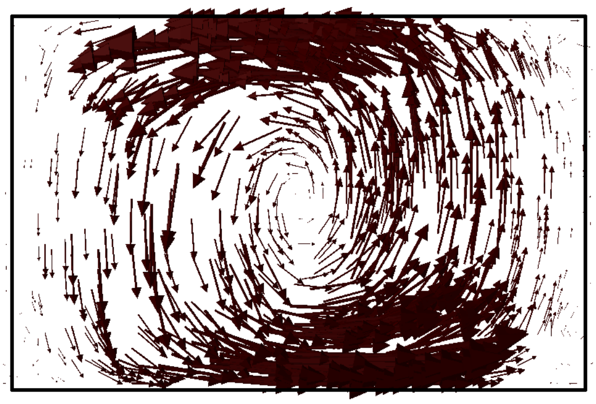

FIG. 7.4. *Distribution of eddy current density on the cross-section of the lamination stack at* $x_1 = 0.0057$.

8. Concluding remarks. We study the homogenization of multi-scale time-dependent electromagnetic eddy current problems in three dimension. The homogenized $\boldsymbol{H}$-formulation is proposed for nonlinear problems and multiply-connected conductors. For nonmagnetic materials, the homogenized Maxwell's equations are also derived by linking up the $\boldsymbol{H}$-formulation and the $\boldsymbol{A}$-formulation. The homogenized eddy current model is validated by finite element computing of an engineering benchmark problem from the International Compumag Society.

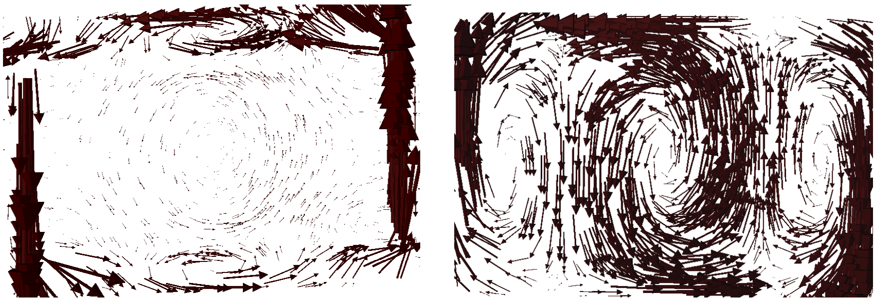

FIG. 7.5. *Distribution of eddy current density on two cross-sections of the magnetic plate. Left: the side adjacent to the lamination stack. Right: the opposite side.*

Acknowledgement. The authors thank the anonymous referees very much for their valuable suggestions and comments on this paper, particularly for the suggestion to extend the contents of numerical computations.

REFERENCES

[1] H. Ammari, A. Buffa, and J. Nédélec, *A justification of eddy current model for the maxwell equations*, SIAM J. Appl. Math., 60 (2000), pp. 1805–1823.

[2] C. Amrouche, C. Bernardi, M. Dauge, and V. Girault, *Vector potentials in three-dimensional non-smooth domains*, Math. Meth. Appl. Sci., 21 (1998), pp. 823–864.

[3] F. Bachinger, U. Langer, J. Schöberl, *Numerical Analysis of Nonlinear Multiharmonic Eddy Current Problems*, Numer. Math., 100 (2005), pp. 593-616.

[4] R. Beck, R. Hiptmair, R. Hoppe and B. Wohlmuth, *Residual based a posteriori error estimators for eddy current computation*, Math. Model. Numer. Anal. 34 (2000), pp. 159–182.

[5] A.J. Bergqvist and S.G. Engdahl, *A homogenization procedure of field quantities in laminated electric steel*, IEEE Trans. Magn., 37 (2001), no. 5, pp. 3329-3331.

[6] A. Bermúdez, D. Gómez, and P. Salgado, *Eddy-current losses in laminated cores and the computation of an equivalent conductivity*, IEEE Trans. Magn., 44 (2008), no. 12, pp. 4730-4738.

[7] O. Bottauscio, V. Chiadopiat, M. Chiampi, M. Codegone, and A. Manzin, *Nonlinear homogenization technique for saturable soft magnetic composites*, IEEE Trans. Magn., 44 (2008), no. 11, pp. 2955-2958.

[8] O. Bottauscio, M. Chiampi, and A. Manzin, *Homogenized magnetic properties of heterogeneous anisotropic structures including nonlinear media*, IEEE Trans. Magn., 45 (2009), no. 3, pp. 1276-1279.

[9] L. Cao, Y. Zhang, W. Allegretto, and Y. Lin, *Multiscale asymptotic method for Maxwell's equations in composite materials*, SIAM J. Numer. Anal., 47 (2010), pp. 4257-4289.

[10] Z. Cheng, N. Takahashi, and B. Forghani, *TEAM Problem 21 Family (V. 2009)*, approved by the International Compumag Society Board at Compumag-2009, Florianópolis, Brazil, http://www.compumag.org/jsite/team.html .

[11] Z.Cheng, N.Takahashi, B. Forghani, and et al, *Electromagnetic and Thermal field Modeling and Application in Electrical Engineering*, Science Press, Beijing, 2009.

[12] J. Chen, Z. Chen, T. Cui and L. Zhang, *An adaptive finite element method for the eddy current model with circuit/field couplings*, SIAM J. Sci. Comput., 32 (2010), pp. 1020-1042.

[13] M. Costabel, M. Dauge, and S. Nicaise, *Singularities of eddy current problems*, ESAIM: Mathematical Modelling and Numerical Analysis, 37 (2003), pp. 807–831.

[14] J. Gyselinck and P. Dular, *A time-domain homogenization technique for laminated iron cores in 3D finite element models*, IEEE Trans. Magn., 40 (2004), no. 3, pp. 1424-1427.

[15] J. Gyselinck, R.V. Sabariego, and P. Dular, *A nonlinear time-domain homogenization technique for laminated iron cores in three-dimensional finite-element models*, IEEE Trans. Magn., 42 (2006), pp. 763-766.

[16] V. E. Henson and U. M. Yang, *BoomerAMG: a parallel algebraic multigrid solver and preconditioner*, Appl. Num. Math., 41 (2002), pp. 155-177.

[17] N. Hihat, E. Napieralska-Juszczak, J.-P. Lecointe, J.K. Sykulski, and K. Komeza, *Equivalent permeability of step-lap joints of transformer cores: computational and experimental considerations*, IEEE Trans. Magn., 47 (2011), no. 1, pp. 244-251.
[18] R. Hiptmair, *Analysis of multilevel methods for eddy current problems*, Math. Comp., 72 (2002), pp. 1281–1303.
[19] X. Jiang and W. Zheng, *An efficient eddy current model for nonlinear Maxwell equations with laminated conductors*, SIAM J. Appl. Math., 72 (2012), pp. 1021–1040.
[20] H. Kaimori, A. Kameari, and K. Fujiwara, *FEM computation of magnetic field and iron loss using homogenization method*, IEEE Trans. on Magnetics, 43 (2007), no. 2, pp. 1405-1408.
[21] P.D. Ledger, and S. Zaglmayr, *hp-Finite element simulation of three-dimensional eddy current problems on multiply connected domains*, 199 (2010), pp. 3386-3401.
[22] P. Li, and W. Zheng, *An $\boldsymbol{H}$-ψ formulation for the three-dimensional eddy current problem in laminated structures*, J. Diff. Eqn., 254 (2013), pp. 3476-3500.
[23] J.C. Nédélec and S. Wolf, *Homogenization of the problem of eddy currents in a transformer core*, SIAM J. Numer. Anal., 26 (1989), pp. 1407-1424.
[24] T. Roubíček, Nonlinear partial differential equations with applications, Birkhäuser Verlag, Basel, 2005.
[25] I. Sebestyen, S. Gyimothy, J. Pavo, and O. Biro, *Calculation of losses in laminated ferromagnetic materials*, IEEE Trans. on Magnetics, 40 (2004), no. 2, pp. 924-927.
[26] L. Zhang, *A Parallel Algorithm for Adaptive Local Refinement of Tetrahedral Meshes Using Bisection*, Numer. Math.: Theor. Method Appl., 2 (2009) pp. 65-89.
[27] Y. Zhang, L. Cao, and Y. Wong, *Multiscale Computations for 3D Time-Dependent Maxwell's Equations in Composite Materials*, SIAM J. Sci. Comput., 32 (2010), pp. 2560C2583.
[28] W. Zheng, Z. Chen, and L. Wang, *An adaptive finite element method for the $\boldsymbol{H}$-ψ formulation of time-dependent eddy current problems*, Numer. Math., 103 (2006), pp. 667–689.
[29] W. Zheng and Z. Cheng, *An inner-constrained separation technique for 3D finite element modeling of GO silicon steel laminations*, IEEE Trans. Magn., 12 (2012), pp. 667–689.